Osman *et al. Int J Concr Struct Mater (2025) 19:45*
https://doi.org/10.1186/s40069-025-00777-1

International Journal of Concrete Structures and Materials

RESEARCH Open Access

Flexural Strengthening of Reinforced Concrete Beams with Substandard Tension Lap Splices Using a Novel Pre-stressing Technique

Roba Osman[1], Ahmed Elkhouly[1], Boshra Eltaly[1*] and Mohamed H. Zakaria[2]

Abstract

Sudden failure of reinforced concrete (RC) beams with substandard tension lap splices due to low resistance to flexure is a critical issue that needs to be addressed. Accordingly, a novel pre-stressing technique is presented in this paper, which offers a promising solution for strengthening RC beams with substandard tension lap splices. The technique involves the use of external steel bolts, load-transferring brackets, and bearing plates. Eleven test specimens sized 100×200×1500 mm^3 were utilized in a series of experimental investigations to assess the effectiveness of the suggested approach. These specimens consisted of one specimen without a tension lap splice, one with a sufficient tension lap splice equal to $60d_b$, and nine beams with insufficient tension lap splices equal to $25d_b$. The investigation considered three main variables for eight strengthened specimens: the length of the strengthening plate (L_s=$60d_b$, $80d_b$, and $100d_b$), the number of bolts (N_b=2, 3, and 4 pairs), and the pre-stress level in the bolts (PL=$0.1f_y$, $0.2f_y$, and $0.3f_y$). The effects of the proposed strengthening technique on ultimate load (P_{ult}), first cracking load (Pc), deformation behavior, failure pattern, cracks distribution, deflection ductility, flexure toughness, and elastic stiffness were investigated. The findings demonstrated that the pre-stress approach considerably enhanced the ultimate load (61.52–218.65%) and first crack load (80.15–106.40%) of the strengthened specimens compared with the control specimen. In addition, there was a notable improvement in flexural toughness and elastic stiffness, with an average value of 205.5% and 101.35% for all strengthened specimens, respectively. Also, strengthened RC beams showed considerable improvements in ductility, with an average increase in peak (μ_p) and ultimate deflection (μ_{uf}) indices of 120.16% and 94%, respectively. In general, the novel pre-stressing technique enhances the structural performance of the beams by increasing their load-carrying capacity, improving ductility, and enhancing crack resistance.

Article highlights

- A novel pre-stressing method with external steel bolts, load-transferring brackets, and bearing plates.
- Quick application without hydraulic jacks or adhesives.
- Strengthened beams show enhanced load capacity, ductility, and crack resistance.
- Insights for structural rehabilitation and retrofitting.

Keywords Reinforced concrete beams, Substandard tension lap splices, Pre-stressing technique, Flexural toughness, Elastic stiffness, Load-carrying capacity, Ductility

Journal information: ISSN 1976-0485/eISSN 2234-1315.

*Correspondence:
Boshra Eltaly
boushra_eltaly@yahoo.com
Full list of author information is available at the end of the article

1 Introduction

Rebar splicing is a critical component of reinforced concrete construction, essential for ensuring structural integrity in elements, where the length of reinforcing bars is insufficient to span the entire distance required (Mabrouk & Mounir, 2018; Metelli et al., 2015). Various factors, such as transportation constraints and site conditions, can complicate the use of long reinforcement bars, making effective splicing techniques necessary (Fayed et al., 2023; Mabrouk & Mounir, 2018; Tarabia et al., 2016). Among the various splicing methods, the lap splice is the most commonly used due to its economic efficiency and effectiveness (ACI Committee408, 2003; Najafgholipour et al., 2018). This method involves overlapping two parallel rebars and securing them together using clamping devices or wire ties, allowing for proper load transfer between the bars. Design codes and engineering standards specify the required overlap length to ensure adequate bond strength and load distribution between the spliced rebars (Hasan et al., 2015). Lap splices can be categorized into two main types: contacting splices, where the bars are in direct contact, and non-contacting splices, which allow for a gap between the overlapping bars (Masud et al., 2020).

In addition to the lap splice, there are other methods for rebar splicing. These include mechanical splices (using couplers, sleeves, or connectors), welded splices (where the rebars are welded together), and grouted splices (where the gap between the rebars is filled with grout) (Dabiri et al., 2022; Fayed et al., 2023). Various parameters influence the performance of lap splices in reinforced concrete structures. These parameters include the lapped length (overlap length of the rebars), concrete cover (distance between the rebars and the outer surface of the concrete), lapped rebar percentage, reinforcement rebar diameter, consideration of transverse reinforcement near the splice, bundles wires criteria, concrete mechanical properties, and the location of casting (ACI318, 2019; Al-Quraishi et al., 2019; Haefliger et al., 2022).

In addition to the previously mentioned factors, several other critical elements influence lap splice performance (Croppi et al., 2024; Fayed et al., 2023; Gillani et al., 2021). The surface characteristics of reinforcing bars, such as ribbing or coating, play a significant role in bond strength. The bond strength of injection mortars used in post-installed splices is also important. Furthermore, environmental conditions, including temperature and humidity, can affect splice performance. Loading conditions, such as static versus dynamic loads, may lead to different behaviors in lap splices. Finally, the depth of concrete filling is crucial, as splices in sections less than 6 inches thick may behave differently compared to those in thicker sections due to variations in confinement.

The structural performance of reinforced concrete structures depends critically on the bond behavior between the reinforcing steel and the surrounding concrete (Alharbi et al., 2021). It affects the load transfer mechanism, crack development, and overall structural integrity. There are minimal inadequacies in load-carrying capacity and deformability under lateral loading when the lap splice length is applied in accordance with RC design guidelines (Akın et al., 2022; Verderame et al., 2008). In situations when the retrofit might be more cost-effectively executed in phases, such as when reinforcing large spans or bridge beams that span several lanes of traffic, splicing becomes particularly useful (Kadhim et al., 2021). Nevertheless, the structural element's strength and ductility are weakened when the lap splice length is inadequate (Almeida et al., 2017). Certain areas in reinforced concrete structures require special attention to bond behavior due to higher stress concentrations or complex loadings. Some examples of such regions include contra flexure points or continuous supports, deep beam supports, beam–column connections, and mid-span zones of simply supported beams (Dabiri et al., 2022; Fayed et al., 2023). The term "substandard bonded length" refers to an embedded length that falls short of the minimum distance required by the code (Akın et al., 2022). As to the Egyptian Code, the appropriate length for reinforcing bars under tension is 40–60 times d_b, while for compression, it is 20–40 times d_b (E.C.P203–, 2018; Fayed et al., 2023).

There has been extensive global utilization of reinforced concrete constructions. Much of the present-day structures have been constructed throughout the middle of the previous century. During that time, there was a marked shift in the need for designs, while the function of some structures was altered. Consequently, a number of structures fail to satisfy the criteria for serviceability, strength, and ductility set by contemporary standards such as poor design in existing structures including reinforcement details at the splice zones (Dagenais & Massicotte, 2015; Karkarna et al., 2023). In addition, lap splices can need strengthening because of inadequate bonding caused by a variety of factors, including mistakes in design and construction (Makhlouf, 2019; Mousavi et al., 2022). The need for rehabilitation or strengthening of concrete structural components arises periodically across the world for various causes, including incorrect design or construction, rehabilitation or strengthening, increasing service loads, and others (Alexander et al., 2008; Bhattacharjee, 2016). A variety of materials and methods have been employed in recent years to strengthen and renovate existing reinforced concrete structures. Concrete or

steel jacketing technique, externally bonded reinforcement (EBR) such as a fiber-reinforced polymer (FRP) and engineered cementitious composite (ECC), external pre-stressing, near-surface mounted, fiber-reinforced composited materials, and EBR on grooves (EBROG) are commonly available retrofitting schemes (Abdallah et al., 2024; Siddika et al., 2020; Heiza et al., 2014).

To increase the flexural, shear, torsional, and axial sectional capacity of reinforced concrete structural components as well as to offer extra confinement and enhance the stability and serviceability of structural parts, externally bonded reinforcing systems, or EBRs, are employed (Naser et al., 2019). Typically, two basic kinds of strengthening systems are used: one utilizes near-surface mounted (NSM) bars, and the other utilizes plates and/or sheets made of materials like carbon fibers (CFRP) or glass fibers (GFRP) (Makhlouf, 2019). Fixing strengthening sheets or plates to the tension side of the RC beam is the fundamental application of the EBR method for flexural strengthening. Comprehensive research was done on the failure mechanisms and behaviors of the RC beams strengthened by EB. The most prevalent and predictable failure mechanism is the soffit material plate's intermediate crack-induced debonding, also known as IC debonding (Teng et al., 2003; Yang et al., 2022). Due to this failure pattern, the ultimate strength of strengthened beams is determined by regulations or standards in many countries (Aiello et al., 2014; ACI440, 2002; CSA, 2002; Maruyama, 2001). When the IC debonding failure mode occurs, the strength of the bond between the EBR and the concrete determines the beam's maximum allowable strength (Smith & Teng, 2002), and the EBR is usually at a low-stress level at the ultimate state. To forecast the EBR–concrete interface's behavior, two models are suggested: bond-slip and bond-strength (Chen et al., 2011, 2015). EB debonding not only induces early brittle failure but also restricts the enhancement of beam stiffness in the serviceability limit state. This is due to the fact that the stress activation occurs only after crack propagation on the concrete beam (Oehlers et al., 2013). In accordance with the results of previous EBR investigations, Table 1 offers a comprehensive comparison. It is worth noting that the majority of prior research was carried out using embedded lengths that ranged from 5 to 40 times the diameter of the bar. These lengths were determined to be less than the standard bonded length as specified by national regulations/codes.

While previous research has highlighted the considerable benefits of employing externally bonded systems (EBRs) to strengthen concrete beams (Abdalla et al., 2020; Foraboschi, 2022; Salmi, 2024; Slaitas, 2024; Taie et al., 2024), their widespread adoption is impeded by several challenges associated with the lack of clarity regarding the durability of EBR-based repairs. Considerations about the durability of the composite-to-structure bond under harsh environmental conditions, including freeze–thaw cycles, high temperatures, and dry–wet conditions, are important when considering the use of EBR for civil structure repair (Albuja-Sánchez et al., 2024; Kadhim et al., 2021; Subramaniam et al., 2008). To address the drawbacks of the EB method, other alternatives have been considered and investigated. Improving the bond quality is the first strategy. By using the near-surface mounted (NSM) method, strips or rods are affixed to the concrete surface via grooves (De Lorenzis & Teng, 2007). For design and analysis, bond strength and bond-slip models were also suggested (Zhang & Teng, 2013). To further improve the bond quality, anchors may be placed on the bonded interface to provide additional anchorages (Yang et al., 2018). Furthermore, confinement serves to diminish the deterioration of the steel reinforcement's bond and restricts the extent of damage to the concrete inside the confined area. Consequently, this results in an enhanced capacity of the structure to absorb and dissipate energy (Harajli, 2009).

Employing the pre-stress technique is another crucial method for enhancing the effectiveness of strengthening (Aslam et al., 2015; Seręga & Faustmann, 2022). In combination with EB or NSM approaches, the pre-stress system may be pre-tensioned, post-tensioned, or anchoring systems may be implemented concurrently (Wang et al., 2012, 2013). Two fixed anchors are included in the strengthening system in addition to a tensioning mechanism. Applying epoxy glue to the bond surface comes before pre-stressing. To apply the tension stress, a hydraulic jack is then positioned between the fixed anchor and the response plate. Once the desired level of jacking force is achieved, the nuts inside the tensioning device are securely tightened. When the hydraulic jack is finally released, the plate's stress is controlled by the two fixed anchors. Despite ongoing approval, this approach needs further improvement (Seręga & Faustmann, 2022; Yang et al., 2022). First, there is a restriction on design flexibility due to the size of the tensioning device. A short pre-stressed beam length could cause local shear failure if the tensioning mechanism is too close to the beam support. Second, the application of the strengthening technique requires epoxy adhesives, which generally have a curing period of at least 72 h (Wang et al., 2012, 2013). This curing time might lead to negative externalities, particularly when it comes to strengthening transportation infrastructures. In a related context, Hussein et al. (2013) proposed a novel technique for shear strengthening of reinforced concrete (RC) beams using carbon fiber-reinforced polymer (CFRP) sheets, which involves applying a temporary compressive force parallel to the beam depth

Table 1 Summary of earlier investigations on external strengthening techniques of reinforced concrete elements with substandard lap splices

References	Element type	Number of observations	Test configuration	Length of TLS	Employed method	Δ*P* (%)
Tepfers (1988)	Beams with TLS	10	4-Point flexural test	$32.2d_b$	Spiral confining	Approx. 50%
Melek et al. (2003)	Columns	12	Cyclic loading	$20d_b$	Confined with steel stirrups at splice regions	50–60%
Hamad et al., (2004a, 2004b)	Beams with TLS	22	4-Point flexural test	$20–30d_b$	GFRP wrap	8–34%
Breña and Schlick (2007), Bousias et al. (2007), Karayannis et al. (2008)	Columns with TLS in full-scale	34	Cyclic loading	$20–25d_b$	Confined with FRP layers at splice regions	30–70%
Bournas and Triantafillou (2011)	Columns	6		$20d_b$	Composite jacket confinement (FRP and textile reinforced mesh—TRM)	Approx. 35%
Garcia et al., (2014, 2015)	Beams with TLS	20	4-Point flexural test	$25d_b$	Externally confined using steel stirrups and/or CFRP sheets	14–65%
Helal et al. (2016)		10		$10d_b$	Post-tension method utilizing strap (PTMS) at splice regions	58%
Makhlouf (2019)		12		$26.67–45.80d_b$	NSM stirrups, CFRP, and GFRP strip layers (lengths: 45.80 to $66.67d_b$)	9.70–117%
Etman et al. (2019)		9		20, 30, and $55d_b$	Jacketing of UHP–SHCC with embedded vertical stirrups	6–57%
Assaad (2021)	Pull-out	32	Both monotonic eccentric and central pull-out loading tests	$5d_b$	Internal confinement by stirrups and external confinement by CFRP sheets, and a combination of the two methods	Approx. 40%
Mousavi et al. (2022)	Beams with TLS	8	4-Point flexural test	$16.67d_b$	NSM and NSM–CFRP confinement methods	19.95–46.76%
Ejaz et al. (2022)		19		$20–35d_b$	Hollow steel section (HSS) collars	10.3–82.6%
Elsanadedy et al. (2023)		22		$40d_b$	Externally attached CFRP (carbon FRP) U-wraps versus confining steel stirrups	Up to 106%
Abbas et al. (2023)		6		$65d_b$	Full-scale glass FRP (GFRP) reinforced beam	2–30%
Abdallah et al. (2024)		11		$10d_b$	ECC ferrocement layers (lengths: $60d_b$, $80d_b$, and $100d_b$)	114–164%

where d_b is the main steel diameter of bar reinforcement. GFRP: Glass Fibre Reinforced Concrete; CFRP: Carbon Fiber Reinforced Polymer; SFRC: Steel Fiber Reinforced Concrete; NSM: Near Surface Mounted; UHPC: Ultra-High-Performance Concrete; FRC: Fiber Reinforced Concrete; FRP: Fiber Reinforced Polymers; ECC: Engineered Cementitious Composite; UHP-SHCC: Ultra-High-Performance Strain Hardening Cementitious Composites; TLS: tension lap splice. Δ*P* is the increase ratio in the strength due to strengthening

in the cracking shear zone prior to CFRP installation. This approach aims to close existing shear cracks, generate tension in the CFRP strips upon force removal, and develop compression in the internal stirrups, thereby delaying crack formation and improving the effectiveness of the strengthening system. The authors validated their technique through experimental testing on seven RC beams and compared the results with predictions from existing guidelines, demonstrating the potential advantages of this novel strengthening method over conventional CFRP strengthening approaches. The review by Albuja-Sánchez et al. (2024) evaluates various fiber-reinforced polymers (FRPs) used in civil infrastructure, including CFRP, BFRP, GFRP, and natural FRPs. It highlights the superior mechanical properties of CFRP while noting the cost-effectiveness and environmental

advantages of BFRP and GFRP. The review summarizes experimental studies demonstrating the effectiveness of FRPs in strengthening structures, resulting in improved load capacity and ductility. It also discusses challenges such as bonding issues and the need for standardized guidelines, and suggests future research directions to enhance the performance and sustainability of FRP applications in infrastructure.

Based on the literature review, using the pre-stressing technique, minimal studies have dealt with strengthening reinforced concrete beams, especially those with substandard tension lap splices. In addition, to further improve and eliminate the drawbacks of the aforementioned strengthening systems, the paper aims to strengthen reinforced concrete beams with substandard tension lap splices using a novel pre-stressing technique. The technique involves the use of bolts, load-transferring brackets, and bearing plates, and it is designed to be fast and easy to apply without the need for hydraulic jacks or adhesive materials. To evaluate the effectiveness of the proposed method, a series of experimental tests were conducted using eleven test specimens. These specimens consisted of one beam without a tension lap splice, one with a tension lap splice equal to $60d_b$, and nine beams with tension lap splices equal to $25d_b$. The investigation considered three main variables: the length of the strengthening plate (L_s), the number of bolts (N_b), and the pre-stress level in the bolts (PL).

Table 2 Mix proportions of normal concrete

Water	Cement (C)	Sand	Basalt dolomite	Superplasticizer	Water–cement ratio (W/C)
kg/m^3					–
150	300	650	1290	2	0.50

2 Experimental Testing Program

2.1 Materials

2.1.1 Concrete

Normal concrete (NC) has been employed to cast eleven RC beams. NC was composed, as stated in Table 2, of the following: sand as the fine aggregate, graded crushed basalt dolomite with a maximum nominal size of 15 mm as the coarse aggregate, 42.5 grade Portland cement, water, and superplasticizer. The grain size distribution curves of the employed fine and coarse aggregates are shown in Fig. 1. Table 3 details the physical specifications of the NC components. By using Sikament-163 M as a superplasticizer, the workability of fresh concrete was enhanced. The superplasticizer used in our concrete mix is primarily based on polycarboxylate ether (PCE). The chemical structure of PCE includes a backbone of polyethylene glycol (PEG) that is modified with carboxylic acid groups.The superplasticizer's composition includes 72% active components (comprising PEG and carboxylic acid groups) and 28% water. This formulation is designed to ensure optimal performance in enhancing the properties of the concrete. The active components facilitate improved dispersion of cement particles, which in turn enhances workability and reduces the water–cement ratio without compromising the mix's consistency.

The water-to-cement ratio was 0.5. The concrete compressive strength was determined from $150\times150\times150$

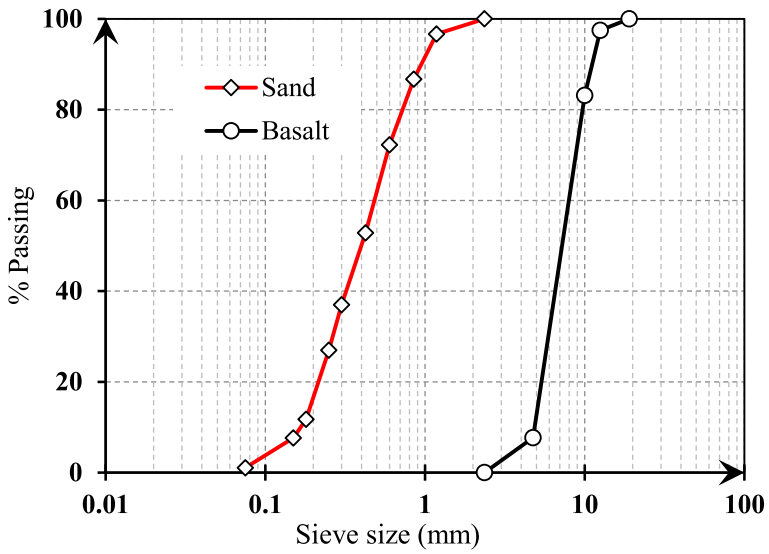

Fig. 1 Particle size distribution of sand and basalt used

Table 3 Physical properties of basalt, sand, and cement

Material	Maximum nominal size		Fineness modulus	Unit weight (kg/m^3)	Specific weight
	Diameter (mm)	Percentage (%)			
Basalt	15	2.51	2.11	1233.7	2.43
Sand	1.18	3.34	6.07	1302	2.67
Cement	0.075	13.8	NA	1206	3.13

mm^3 concrete cubes taken from the mix, which had an average 28-day compressive strength of 30 MPa. As well as three cylinders (150×300 mm^2) were taken to specify its tensile splitting strength.

2.1.2 Internal Reinforcing Steel

In this study, normal mild steel (NMS) and high tensile steel (HTS) were used as internal steel rebars. NMS was a circular bar with a smooth surface and 8.0 mm diameter. Meanwhile, HTS was a circular bar with ribs on its surface and was 10.0 mm in diameter. For casted beams, NMS was used as secondary reinforcement as well as transversal reinforcement (stirrups), while HTS was employed as primary reinforcement. To ascertain the employed steel bars' mechanical characteristics, tension tests were carried out. The stress–strain curves for both NMS and HTS bars and the tension test are shown in Fig. 2.

2.1.3 External Pre-stressed System

The proposed technique consists of bolts, load-transferring brackets, and a pair of bearing plates. All these parts are made of steel. Fig. 3 indicates the components of the proposed strengthening system. Mild steel bolts with a diameter of 6.0 mm and a yield stress of 270 MPa have been used (Fig. 3). The dimensions of the load-transferring brackets were 50×10×220 mm^3. In addition, the load-bearing plates were 100 mm in width and 8 mm in thickness and employed in three different lengths: 600, 800, and 1000 mm (60db, 80db, and 100db), with a yield stress of 350 MPa. The 8 mm thickness of the plates was chosen to balance strength, durability, and manufacturability. This plate is necessary to withstand the anticipated loads and enhance the structural integrity of the beams being reinforced. The added weight increases the self-weight of the member; however, the benefits gained in terms of strength and performance significantly outweigh the drawbacks. Fig. 3 depicts the stress–strain curves of the bolts and the load-bearing plates.

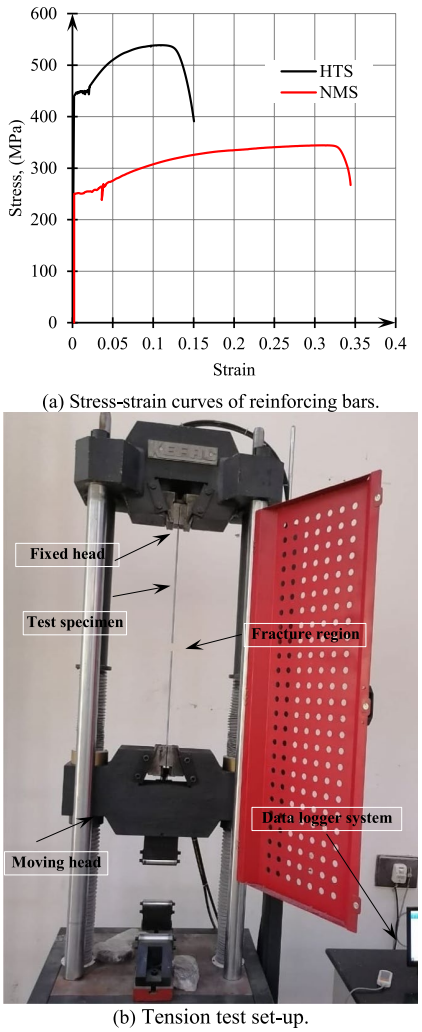

(a) Stress-strain curves of reinforcing bars.

(b) Tension test set-up.

Fig. 2 Tension test of employed steel bars

2.2 Specimen Preparation

The test specimens consist of eleven beams distributed as follows: one specimen without tension lap splice, one specimen with tension lap equal 60d$_b$, and nine specimens with tension lap spliced equal 25d$_b$.

The designation of "substandard" or "insufficient lap length" refers to an embedded length that does not meet the minimum requirements set by relevant codes (Akın et al., 2022). According to the Egyptian Code (E.C.P-203, 2018), the acceptable length for reinforcing bars under

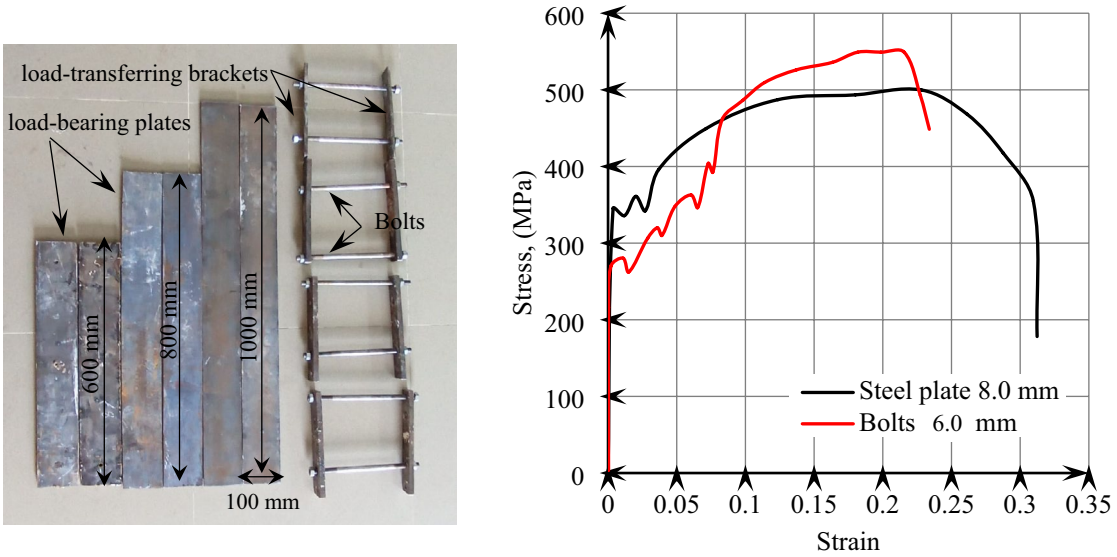

(a) Image from the lab. (b) Stress-strain curves of bolts and plates.

Fig. 3 Components of the pre-stressed technique

tension ranges from 40 to 60 times the bar diameter (db), while for compression, it is 20 to 40 times db.

In this study, a lap splice length of 60db was chosen to represent the minimum adequate length as specified by the Egyptian Code, while the 25db length reflects a common range of insufficient lap lengths found in existing literature. As shown in Table 1, which reviews previous research on the external strengthening of reinforced concrete (RC) beams with insufficient tension lap splices, the range of insufficient lap lengths reported in prior studies varies from 10 to 45db, with a mean of 26.17db and a median of 26.0db. This supports the selection of 25db for our specimens as a representative value of insufficient lap length, allowing us to investigate the effects of both sufficient and insufficient splice lengths. Fig. 4 illustrates the statistical distribution of tension lap splice lengths based on the data compiled in Table 1, further justifying the selection criteria.

Table 4 summarizes the details of specimens and strengthening parameters. According to that, all the studied specimens had the same geometrical dimensions, with 100 mm width, 200 mm depth, and a span of 1500 mm. All the specimens have a 15 mm concrete cover. Two 10 mm-diameter deformed HTS bars were used as bottom reinforcement, whereas two 8.0 mm-diameter smooth NMS bars were used as top reinforcement. Stirrups with a diameter of 8.0 mm were arranged at a center-to-center spacing of 50 mm within the total length of the beam span to prevent the shear failure (Meng et al., 2023). All specimens were classified into four groups. Group G_I consists of five specimens; $B_{C\text{-}0}$ (without lap splice), $B_{C\text{-}L60}$ (with sufficient tension lap = $60d_b$), $B_{C\text{-}L25}$ (with insufficient tension lap = $25d_b$), $B_{C\text{-}P60}$ (with insufficient tension lap = $25d_b$ and strengthened with two plates using adhesive material and shear connectors), and specimens B_1. The purpose of this group is to study the effect of tension lap splice length, as well as to compare external strengthening using the adhesive material and external strengthening proposed pre-stressed technique. The remaining three groups, namely, G_{II}, G_{III}, and G_{IV}, include specimens strengthened using the proposed pre-stressed technique. Each group represents a different combination of variables including the length of the strengthening plate (G_{II}), the number of bolts (G_{III}), and the pre-stress level of bolts (G_{IV}).

Fig. 5 depicts the beams' dimensions and reinforcement details. The specimens were cast by pouring the concrete mixture layer by layer along the vertical axis. This process helps in achieving uniform compaction and eliminates potential voids or air pockets within the concrete. After 24 h, when the concrete had gained sufficient strength, the specimens were carefully removed from the mold. The de-molded specimens were then transferred to a curing room with a controlled environment. This curing room maintained a temperature of 20℃ ± 2℃ and a relative humidity of 95% RH. Following the initial curing period, the specimens were stored in a fog room. The fog room is maintained at a temperature of 23 ± 2℃. This

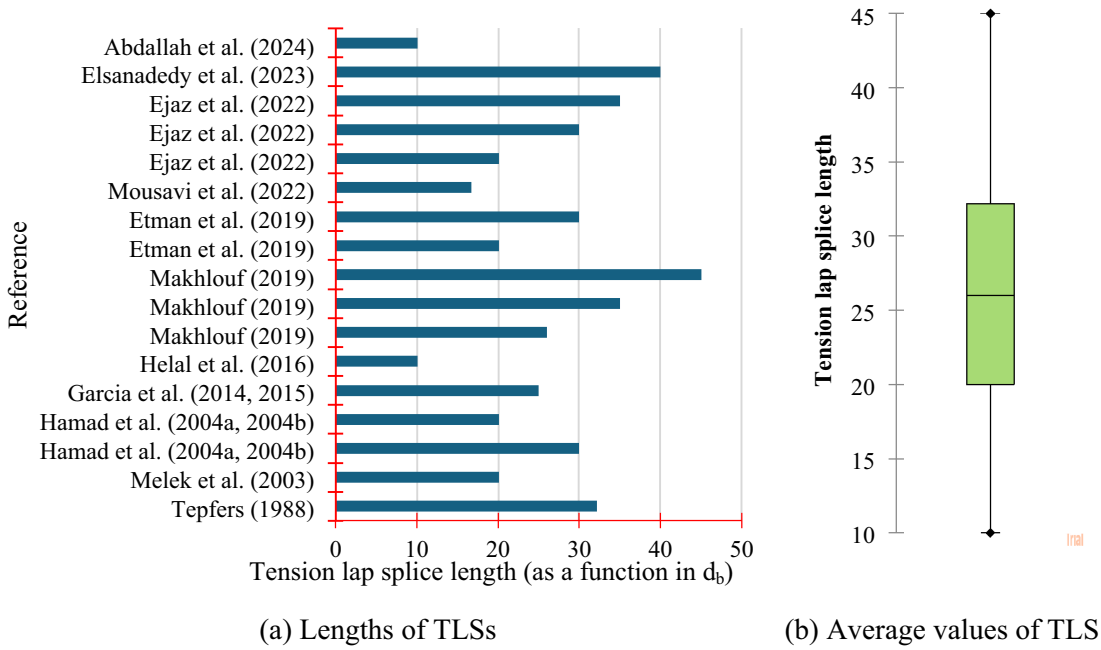

Fig. 4 Statistics and values of insufficient tension lap splices based on previous studies

additional storage period allows for further hydration and the development of strength in the concrete before testing. Fig. 6 indicates images from specimen perpetration.

2.3 Strengthening Procedures

As was already stated, this research study focuses on three main variables. These variables included the length of the strengthening plate (L_s), number of bolts (N_b), and pre-stress level in bolts (PL). The bearing plates are steel plates positioned adjacent to the rebars in the lap zone, typically a fraction of the diameter of the tension rebar (e.g., $60d_b$, $80d_b$, and $100d_b$). The selection of plate lengths (60db, 80db, and 100db) was based on previous research, such as that conducted by Abdallah et al. (2024), which provides a foundation for our choices. The study aimed to align this study with established methods to ensure consistency and comparability in the results. They are typically installed on the top and bottom surfaces of the specimens. The primary function of the bearing plates is to distribute the applied loads more evenly across the surface of the specimen. The bolts are tensioned to a predetermined stress level, typically a fraction of the yield strength of the bolts (e.g., 0.1*fy*, 0.2*fy*, and $0.3f_y$). By applying this pre-stress to the bolts, they generate a compressive force that acts perpendicular to the direction of the tension in the specimen.

For specimen $B_{C\text{-}P60}$, the strengthening plates were bonded to the concrete surface using shear connectors and epoxy resin material (Fig. 7). In this investigation, Kemapoxy 165 epoxy resin was used. As an adhesive mortar, Kemapoxy 165 bonds steel to concrete (Fayed et al., 2022). Kemapoxy 165 has many advantages, including accepted adhesion between steel and concrete, high mechanical strength, high chemical resistance, and no shrinking (Fayed et al., 2022). The specifications of BS EN 12004 (2017), ASTM C 881 (2003), and BS12 (1978) are all met by this adhesive. As shown in Fig. 7, the shear connectors were employed to enhance bonding and prevent sliding. The diameter of the connector is 6 mm, and the length of the straight section is 50 mm. Two identical halves, one threaded and one smooth, make up the 50 mm straight length (Fayed et al., 2022). In accordance with the supplier, these screws have 250 MPa yield strength and are manufactured from NMS. Specimens B_1, B_6, and B_7 had the same strengthening configuration except for the prestress level in the bolts (Fig. 7). The length of the plates for these specimens is 600 mm. Before the strengthening process started, the specimens were examined to make sure their top and bottom surfaces were level and horizontal. Any obstacles affecting the surface's level or the contact between the concrete and the plates were removed.

To achieve the desired prestressing levels of 10%, 20%, and 30% of the yield stress (with a yield stress of 270 MPa for the bolts), calculations were performed to determine the expected pressure under the

Table 4 Details of specimens and strengthening parameters

Number	Group ID	Specimen ID	Specimen dimensions			Steel reinforcement				Strengthening parameters			
			W	D	L	+ ve	−ve	St	Lap splice	Plate length	No. of bolts	Pre-stress level	Notes
			mm			mm			mm	mm	Pairs	–	
1	G_I	$B_{C\text{-}0}$	100	200	1500	2φ10 (deformed HTS bars)	2φ8 (smooth NMS bars)	φ8@ 50 mm (smooth NMS bars)	–	–	–	–	–
2		$B_{C\text{-}L25}$							$25d_b$	–	–	–	–
3		$B_{C\text{-}L60}$							$60d_b$	–	–	–	–
4		$B_{C\text{-}P60}$							$25d_b$	$60d_b$	–	–	AM
5		B_1								$60d_b$	3	$0.1f_y$	–
6	G_{II}	B_2								$80d_b$	3	$0.1f_y$	–
7		B_3								$100d_b$	3	$0.1f_y$	–
8	G_{III}	B_4								$60d_b$	2	$0.1f_y$	–
9		B_5								$60d_b$	4	$0.1f_y$	–
10	G_{IV}	B_6								$60d_b$	3	$0.2f_y$	–
11		B_7								$60d_b$	3	$0.3f_y$	–

where W refers to width, D refers to depth, L refers to length, + ve steel refers to main/bottom reinforcement, −ve steel refers to secondary/top reinforcement, St refers to stirrups, and AM refers to adhesive materials (Kemapoxy 165 and 3 shear connectors for both top and bottom strengthening plate). d_b is the main steel diameter of bar reinforcement. $25d_b$, $60d_b$, $80d_b$, and $100d_b$ are equivalent to 250, 600, 800, and 1000 mm, respectively. $0.1f_y$, $0.2f_y$, and $0.3f_y$ equates to pre-applied stress in each bolt of 27, 54, and 81 MPa, respectively

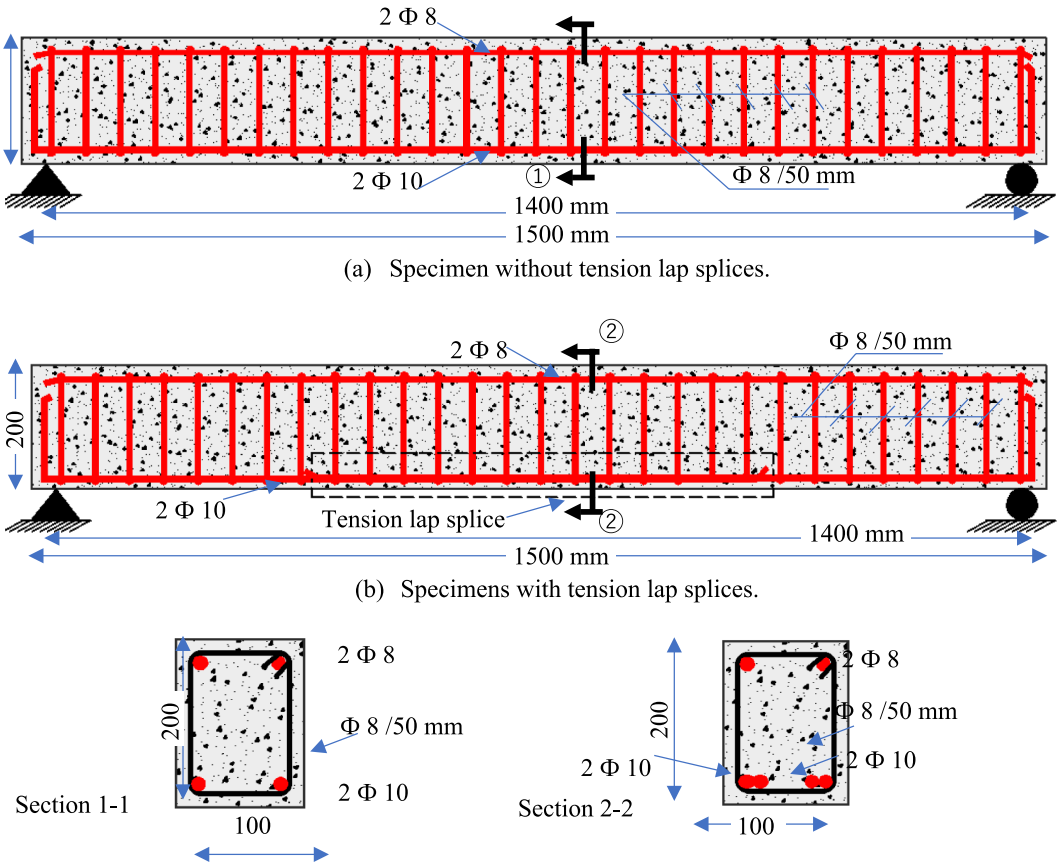

Fig. 5 Beams' dimensions and reinforcement details

loading plates based on the bolt diameter (6 mm), the selected stress levels, and the number of bolt pairs. This approach enables effective determination of the load-to-area ratio.The prestress level in the bolts was confirmed by measuring the pressure beneath the upper and lower bearing plates using small-sized pressure transducers, capable of measuring pressures up to 10 MPa. These transducers were installed under the plates and connected to a data logger, facilitating accurate monitoring of pressure distribution during the application of prestress. Hydraulic torque wrenche was utilized to achieve the necessary tightening of the bolts. This wrenche provides high torque output from a compact tool, operating from a 10,000 PSI hydraulic pump. It offers torque capacities of up to 100,000 ft/lbs while maintaining critical accuracy (± 3%) and repeatability (± 1%).

Considering the previously mentioned precautions, specimens B_2 and B_3 were strengthened, as indicated in Fig. 7, with different plate lengths (800 and 1000 mm, respectively) and the same pre-stress level ($0.1f_y$). In addition, Fig. 7, f shows the strengthening configuration of B_4 and B_5 specimens.

2.4 Testing Setup and Measurements

2.4.1 Compressive Strength Test

In this study, the 28-day compressive strength of the concrete specimens was determined using $150 \times 150 \times 150$ mm^3 cube samples, with an average strength of 30.5 MPa. This value represents the average strength achieved by the concrete after the 28-day curing period.

2.4.2 Tensile Strength Test

The 28-day tensile splitting strengths were examined using 150×300 mm sample cylinders, and the average tensile strength of three 150 mm cylinders was 2.94 MPa.

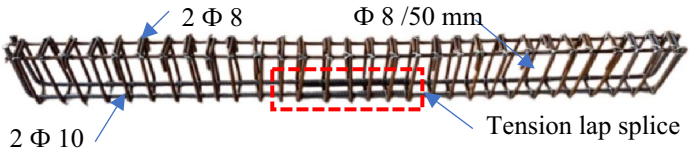

(a) Steel configuration of tension lab spliced specimens.

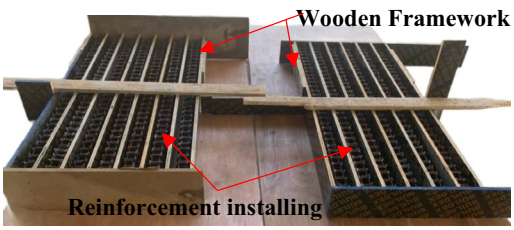

(b) Reinforcements used within the forms.

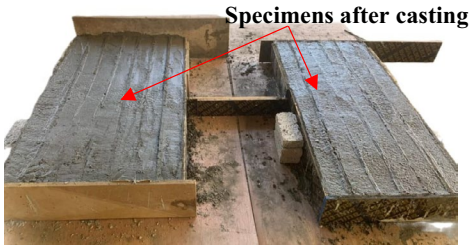

(c) After concrete pouring.

Fig. 6 Images from specimen perpetration

2.4.3 Four-Point Loading Test

A laptop was paired to a UCAM-550A strain data logger device, which automatically captured all test data. To conduct the flexure test, the specimen was placed on a hinge at one end and a rolling support at the other. The force-controlled vertical application of the load was performed using a load cell. Two smooth steel rollers, one-third, and two-thirds of the span apart from one end, transferred the vertical load P from the central span to the specimen (Fig. 8). A linear variable differential transducer (LVDT) was employed to measure the mid-span deflection of the specimen. Fig. 8 depicts the experimental test setup. The loading rate of 0.5 kN/s was used. First crack, failure mode, and the maximum failure load were documented.

3 Test Results and Analysis

3.1 Failure Modes

Fig. 9 illustrates observations on the crack's formation and the failure mechanism of the tested specimens under a four-point loading test. The specimen $B_{C\text{-}0}$, which did not have a tension lap splice, exhibited a particular behavior during the experimental testing. According to Fig. 9, as the load on the specimen gradually increased towards its ultimate value, vertical crack damage started to propagate at the midspan in the tension zone. These cracks then spread out between the two points of loading. This behavior is commonly observed in reinforced concrete beams subjected to bending forces. At the ultimate load, as expected, the failure pattern of the $B_{C\text{-}0}$ specimen was characterized as a typical flexure failure pattern in the pure bending region.

For the specimen with the substandard tension lap-splice region ($B_{C\text{-}L25}$), flexure cracks initially appeared at the ends of the lap zone. These cracks then widened, but their number did not increase significantly. The failure was characterized by a limited number of wide flexural cracks in the concrete near the end of the lap, indicating slippage of the tension rebars, as shown in Fig. 9. This could be explained by the fact that the lap splice length or the embedment length of the rebar is insufficient; accordingly, it led to inadequate bond strength between the rebar and the concrete, resulting in slippage. This slippage can cause a localized stress concentration at the ends of the lap zone, leading to the formation and widening of flexure cracks. The limited number of wide flexural cracks observed in the concrete near the end of the lap zone indicates the occurrence of such slippage.

The findings from this study regarding control samples with sufficient and insufficient lap lengths align well with the results of Teguh and Mahlisani (2016). Their research emphasized the significant impact of lap splice lengths on crack patterns and failure modes. Specifically, control beams in both studies exhibited typical flexural cracking, characterized by cracks originating at the mid-span. For specimens with insufficient lap splice lengths, localized cracking was observed at the ends of the splice due to slippage, indicating a failure in bond strength. Conversely, beams with adequate splice lengths demonstrated extensive and well-distributed cracks, which

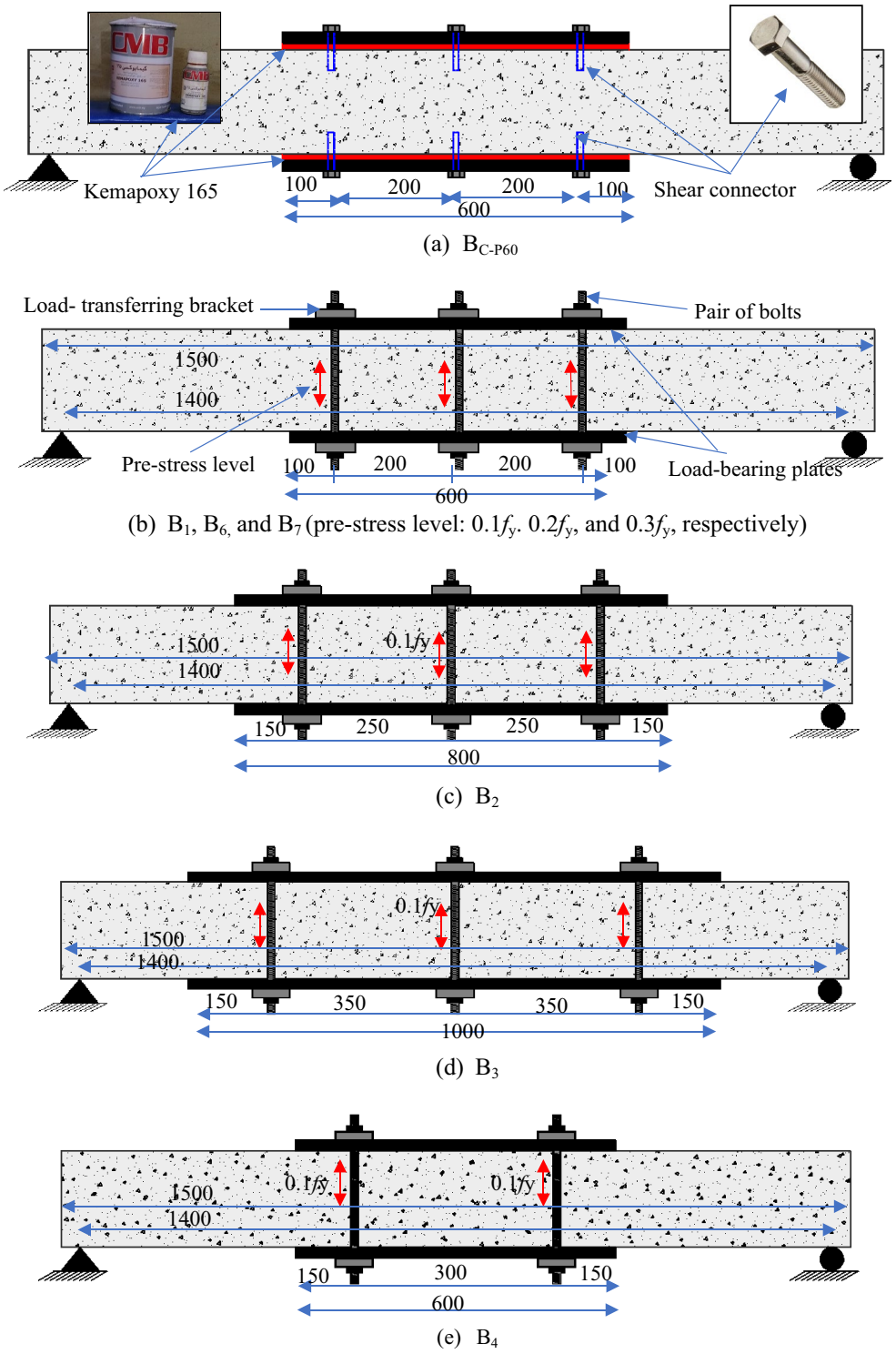

Fig. 7 Strengthening configuration of tested specimens (all dimensions in mm)

highlighted effective load transfer and a more favorable structural performance. This consistency between the studies underscores the critical role of lap splice length in influencing the structural integrity of reinforced concrete beams.

The steel plate strengthening method in specimen $B_{C\text{-}P60}$, which involved adhesive material and shear

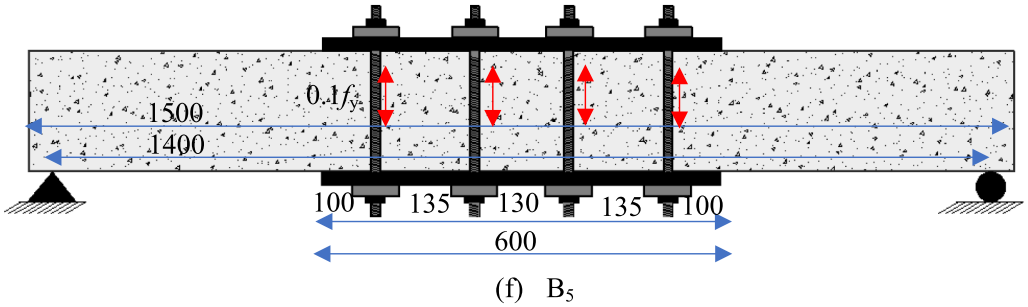

Fig. 7 continued

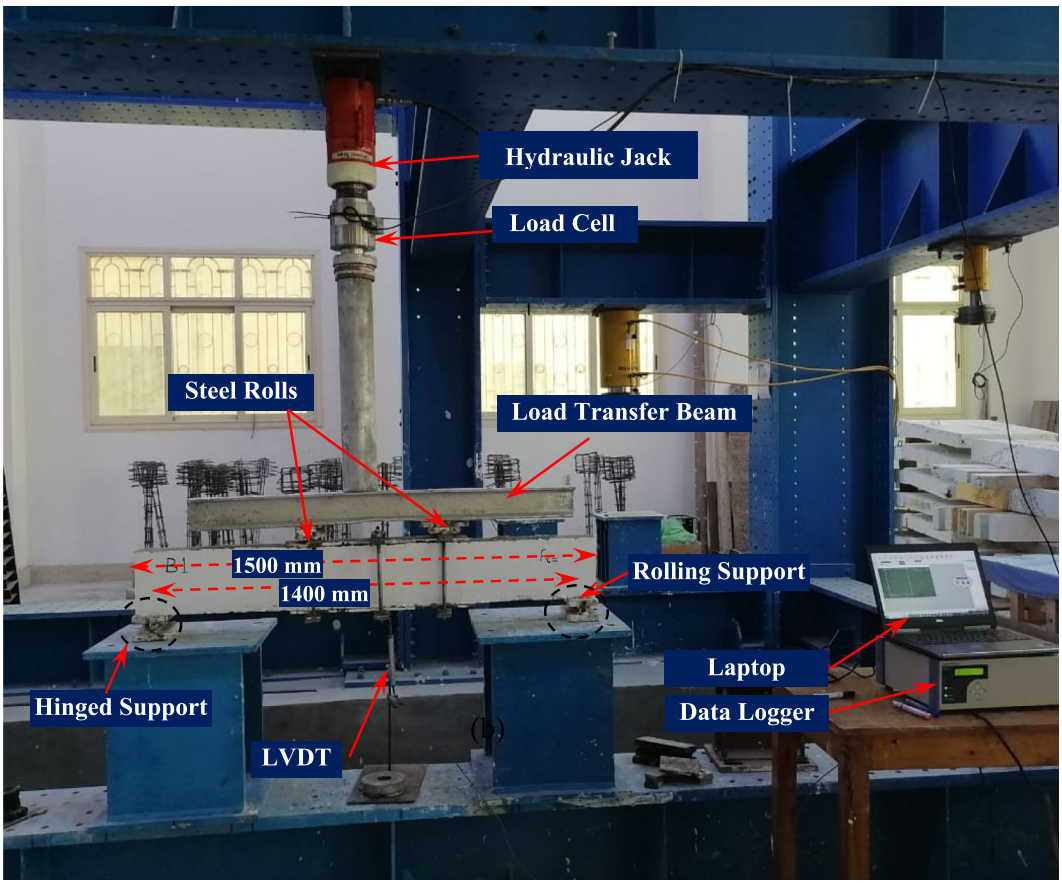

Fig. 8 Four-point loading test setup

connectors, successfully mitigated the slippage of tension rebars in the lap zone. This indicates that the bond between the rebars and the concrete was improved, preventing slippage. However, the failure mode observed in the strengthened specimen was characterized by tensile splitting cracking in the concrete near the ends of the strengthening plates. This cracking resulted in the separation of the concrete cover, as depicted in Fig. 10 of the research paper. The strengthening caused a shifting of the cracked region towards the supports. Although the steel plates themselves did not rupture or fail under the applied load, the concentrated stress near the ends of the plates caused tensile splitting cracking due to the high tensile forces in those regions. This cracking and separation of the concrete cover led to a decline in the load–deflection curve, indicating a reduction in the load-carrying capacity and stiffness of the specimen. The absence of cracks in the midspan of the beam suggests that the steel plates

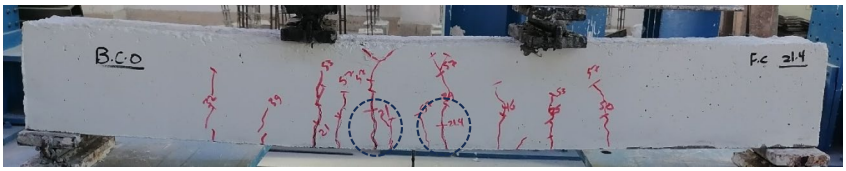

(a) $B_{C\text{-}0}$

(b) $B_{C\text{-}L60}$

(c) $B_{C\text{-}L25}$

Fig. 9 Failure patterns and cracks of tested specimens ($B_{C\text{-}0}$, $B_{C\text{-}L60}$, and $B_{C\text{-}L25}$)

effectively transferred the applied load and prevented flexural cracking in that region. However, the concentrated stress near the ends of the plates resulted in the observed failure mechanism. Elsanadedy et al. (2023) and this study emphasize the critical role of bond strength and stress distribution in influencing crack patterns and failure modes in reinforced concrete beams. In this study, the steel plate strengthening improved load transfer and prevented midspan cracking, while localized tensile splitting occurred at the edges due to concentrated stresses. Similarly, Elsanadedy et al. (2023) highlighted that the initial failure in their beams was related to bond issues, specifically the debonding of CFRP at the free corner, which directly impacted the beam's performance. Both studies demonstrate that adequate bonding is essential for maintaining structural integrity under load.

Flexure cracks initially appeared at the ends of the lap zone in the $B_{C\text{-}L60}$ specimen (Fig. 9). These cracks then propagated towards the tension zone (mid-span) and increased in size and number as the load was increased. In this case, the length of the lap splice did not have a negative effect on the behavior of the specimen; instead, it improved the behavior, because the length of the lap splice was sufficient. An extensive number of wide flexural cracks in the concrete near the end of the lap characterized the failure of the $B_{C\text{-}L60}$ specimen. This pattern of cracks further confirms the flexural failure mode. In summary, the key difference in behavior between the specimen with a sufficient lap splice length ($B_{C\text{-}L60}$) and the one with an insufficient lap splice length ($B_{C\text{-}L25}$) lies in the effectiveness of the bond between the rebars and the concrete. A sufficient lap splice length ensures a stronger bond, leading to improved load transfer and more desirable flexural failure behavior. Conversely, an insufficient lap splice length compromises the bond, resulting in a different failure mode and potentially premature failure.

The proposed pre-stressed technique has proven effective in preventing the slippage of tension rebars in the lap zone. By introducing pre-stressed bolts and bearing plates, the technique has provided additional strengthening to the specimen. In the case of specimen B_1, which utilized a pair of bearing plates measuring 600 mm in length and three pairs of pre-stressed bolts with stress levels equal to $0.1f_y$, the first crack appeared near the edge of the bearing plate (Fig. 10). The stress concentration at the edge of the plate likely influenced this initial crack. Notably, no cracks appeared in the midspan of the beam due to the compression stress exerted by the bearing plates. The compression stress counteracted the tensile stress in this region, preventing the formation of cracks. However, as the vertical load increased, the cracks began to spread and widen towards the supports. The

(a) $B_{C\text{-}P60}$

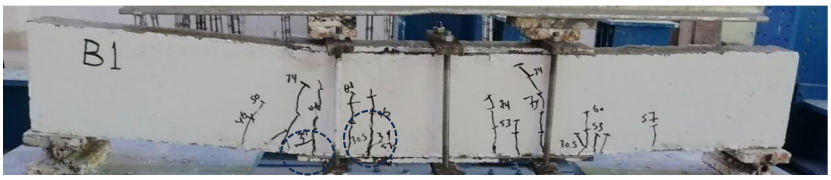

(b) B_1

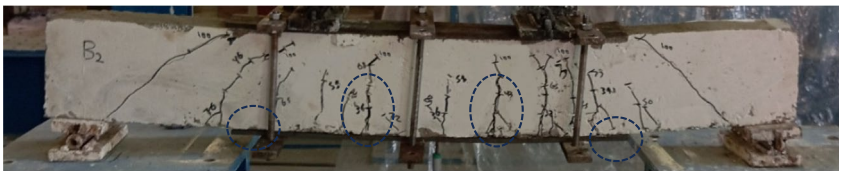

(c) B_2

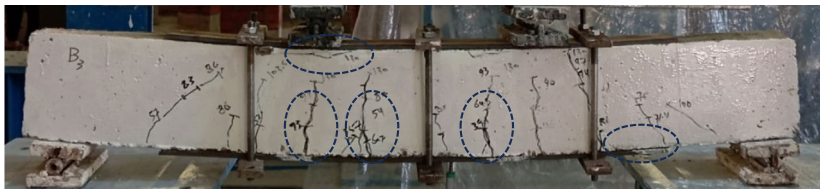

(d) B_3

(e) B_4

Fig. 10 Failure patterns and cracks of tested specimens ($B_{C\text{-}P60}$, B_1 to B_7)

higher load likely exceeded the capacity of the structure to resist bending, leading to the propagation of cracks. The cracks primarily extended from the edge of the bearing plate towards the supports, indicating a shifting of the cracked region. Ultimately, the final failure mode observed was flexure with slipping or small separation of the bottom bearing plate's edges. The failure observed in the specimens utilizing the pre-stressed technique was more ductile than the conventional method. This means that the failure exhibited more deformation and energy absorption capacity before finally reaching the ultimate failure point. When the pre-stressed level in the bolts increased in specimens B_6 and B_7, the initial crack formation occurred at a similar location as in specimen B_1 (Fig. 10). However, there were some notable differences in the crack propagation and failure behavior. First, the ultimate strength of the specimens with increased pre-stressed levels showed a slight improvement compared

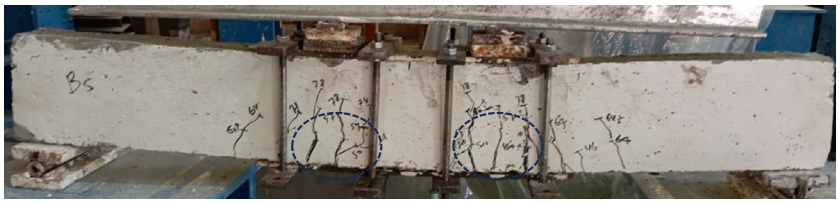

(f) B_5

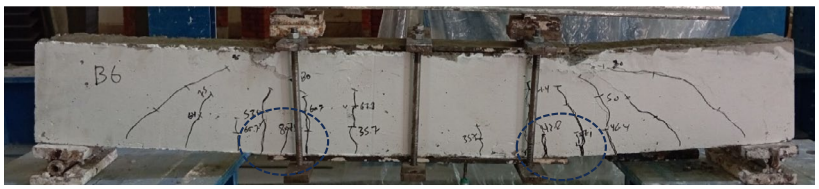

(g) B_6

(h) B_7

Fig. 10 continued

to specimen B_1. The increased pre-stress levels in specimens B_6 and B_7 have improved the load-carrying capacity of the tested beams. As a result, the tested beams were subjected to higher applied loads before reaching their failure point. The increased loads lead to additional cracking and the distribution of cracks over a more considerable beam length. Accordingly, a combination of shear and flexure cracks was observed in specimens B_6 and B_7, in contrast to the predominantly flexural cracks observed in specimen B_1. This indicates that the higher pre-stress levels in the bolts introduced more complex crack mechanisms.

In the case of specimens B_4 and B_5 (Fig. 10), which had different numbers of pairs of bolts but the same pre-stress level of $0.1f_y$, there were some notable differences in their behavior compared to specimen B_1. The presence of more pairs of bolts in specimen B_4 resulted in a stiffer load–deflection curve and prevented the separation of the plate edges during failure. This means it required a higher load to achieve a similar deflection. On the other hand, the larger spacing between the bolts in specimen B_5 led to plate separation and facilitated crack distribution to the mid-span of the beam.

When comparing specimens B_2 and B_3 (Fig. 10), where the length of the bearing plate was increased while maintaining the same pre-stress level of $0.1f_y$, there were several notable effects on the behavior of the specimens. In both specimens B_2 and B_3, cracks formed along the length of the beam, starting from the pure moment region. This means that the initial crack initiation occurred in the area of the highest bending moment. The cracks propagated and extended towards the two supports as the load increased. This behavior is typical in flexural failure modes. The increased length of the bearing plate in specimens B_2 and B_3 resulted in more distributed cracks along the span of the beam compared to other specimens. The extended bearing plate length contributed to a larger area over which cracks could propagate, leading to a wider distribution of cracks. As the ultimate load was approached, the combination of the longer bearing plate length and increased distance between the pairs of bolts led to slippage between the bearing plate and the tested beams. This slippage occurred both in the middle of the span and at the edges. The slippage caused the cracks to widen and increased the number of cracks in the middle span of the beam.

The findings of El-Hacha and Gaafar (2011) regarding the use of prestressed near-surface-mounted CFRP bars demonstrate a clear relationship between prestressing and crack behavior in reinforced concrete beams.

In their study, the strengthened beams exhibited a typical flexural crack pattern, with initial cracks forming at midspan and new cracks appearing at stirrup locations as load increased. The absence of longitudinal cracks at the epoxy–concrete interface indicates the effectiveness of prestressing in maintaining bond integrity. In contrast, the results from the current study highlight a different but complementary approach, focusing on the use of pre-stressed bolts and bearing plates to enhance structural performance. The initial crack in the tested specimens appeared near the edge of the bearing plate, with no midspan cracks due to the counteractive compression stress. While El-Hacha and Gaafar observed failure primarily through the rupture of CFRP bars, the current research identified a more ductile failure mode characterized by a combination of shear and flexural cracks, particularly in specimens with increased pre-stress levels. This suggests that the proposed pre-stressing technique not only improves load-carrying capacity but also alters the crack propagation mechanisms, resulting in a more resilient structural response under loading conditions. Both Rezazadeh et al. (2014) and the current study agree on several key points: both emphasize that prestressing enhances the load-carrying capacity of reinforced concrete beams, leading to improved structural performance. They observe that the predominant crack patterns are flexural in nature, and both highlight that effective bonding between the reinforcement and concrete is crucial for optimal performance, with no instances of debonding reported. In addition, both studies note that prestressing contributes to improved ductility, allowing for greater deformation and energy absorption before failure. Collectively, these findings underscore the critical role of prestressing in enhancing the integrity and performance of reinforced concrete structures, despite employing different reinforcement methods.

3.2 Load–Deflection Relations

The experimental evidence in this section focuses on cracking behaviors and load–deflection relationships of the tested specimens. The load–deflection analysis yielded several important findings, which are summarized in Tables 5 and 6. These findings include parameters, such as ultimate load (P_{ult}), peak mid-span deflection (Δ_p), ultimate final mid-span deflection (Δ_{uf}), first crack load (P_c), and deflection corresponding to P_c (Δ_c), crack patterns, failure type, deflection ductility, flexural toughness (ψ) and elastic stiffness (k).

Furthermore, Fig. 11 displays the load–deflection curves for the four groups. These curves visually represent the relationship between the applied vertical load and the corresponding mid-span deflection for each group. These curves typically exhibit three distinct stages: elastic, elastic–plastic, and softening. In the elastic stage, the load increases linearly with deflection. This stage indicates that the specimen's behavior is initially elastic, meaning it can resist the applied load without significant deformation or damage. As the displacement continues to increase, the load starts to increase nonlinearly, marking the elastic–plastic stage. During this stage, the specimen undergoes deformation and experiences some degree of permanent deformation, indicating a transition

Table 5 Details of critical and ultimate stages

Group ID	Specimen ID	Cracking stage			Ultimate stage			Crack patterns	Failure mode
		P_c	Increase in P_c	Δ_c	P_{ult}	Increase in P_{ult}	Δ_p		
		kN	%	mm	kN	%	mm		
G_I	$B_{C\text{-}0}$	21.6	22.37	1.42	58.11	37.77	7.64	IFC	FF
	$B_{C\text{-}L25}$	17.65	0.00	0.91	42.10	0.00	4.66	IFC	FF + STR
	$B_{C\text{-}L60}$	23.21	31.50	1.39	61.52	46.13	9.12	IFC	FF + STR
	$B_{C\text{-}P60}$	28.45	61.19	1.51	69.05	63.90	9.05	EFC	FF + CCS
G_{II}	B_1	30.57	73.20	1.65	74.12	76.06	9.52	EFC	FF + SSP
	B_2	36.32	105.78	1.15	100.94	139.76	8.44	CSFC	FF + SSP
	B_3	39.6	124.36	0.95	134.15	218.65	6.02	CSFC	FF + SSP
G_{III}	B_4	25.12	42.32	1.81	68.02	61.52	9.41	IFC	FF + SSP
	B_5	39.7	124.93	1.44	78.32	86.03	8.61	EFC	FF
G_{IV}	B_1	30.57	73.20	1.65	74.12	76.06	9.52	EFC	FF + SSP
	B_6	35.5	101.14	1.72	80.46	91.12	13.64	CSFC	FF
	B_7	43.22	144.87	2.01	86.31	105.01	14.48	CSFC	FF

P_{ult} is the ultimate vertical load, Δ_p is mid-span deflection corresponding to peak/ultimate load, P_c is the first cracking load, and Δ_c is the deflection corresponding to P_c. IFC refers to intermediate flexure cracks; STP refers to slippage of tension rebars; SSP refers to limited slipping or separation of the bottom bearing plate; EFC refers to edge flexure cracks; CCS refers to concrete cover separation; CSFC refers to the combination of shear and flexure cracks; and FF refers to flexure failure

Table 6 Details of deformability, ductility ratios, and toughness

Group ID	Specimen ID	Ultimate deflection		Flexure toughness		Elastic stiffness					Ductility		
		Δ_p	Increase in Δ_p	Ψ	ΔΨ	Tan (α)	Δ*k*	Δ_y	Δ_{uf}	μ_{uf}	μ_p	$\Delta\mu_{uf}$	$\Delta\mu_p$
		mm	%	kN.mm	%	–	%	mm	mm	–	–	%	%
G_I	B_{C-0}	7.64	63.95	720	105.71	1.60	27.22	3.4	13.71	4.03	2.25	47.17	39.85
	B_{C-L25}	4.66	0.00	350	0.00	1.26	0.00	2.9	7.95	2.74	1.61	0.00	0.00
	B_{C-L60}	9.12	95.71	905	158.57	1.78	41.67	3.3	15.21	4.60	2.76	68.21	72
	B_{C-P60}	9.05	94.21	930	165.71	1.89	50.00	3.25	15	4.61	2.78	68.44	73.3
G_{II}	B_1	9.52	104.29	1055	201.43	1.92	52.38	3.6	16.70	4.63	2.64	69.30	64.58
	B_2	8.44	81.12	1205	244.29	4.13	227.78	2	14	7.0	4.22	155.47	162.63
	B_3	6.02	29.21	920	162.86	5.32	322.22	1.8	8	4.44	3.34	62.21	108.14
G_{III}	B_4	8.61	84.76	705	101.43	1.56	23.97	4.55	13.8	3.03	1.89	10.58	17.77
	B_5	9.41	101.93	1075	207.14	2.58	105.08	2.15	16.2	7.53	4.38	175.0	172.39
G_{IV}	B_1	9.52	104.29	1055	201.43	1.92	52.38	3.6	16.7	4.63	2.64	69.30	64.58
	B_6	13.64	192.70	1170	234.29	1.96	55.71	3.5	16.8	4.8	3.90	75.18	142.54
	B_7	14.48	210.73	1430	308.57	2.31	83.33	3.3	19	5.75	4.39	110.13	173.08

where μ_p is the peak ductility index; μ_{uf} is the ultimate ductility index; Δ*p* is the mid-span deflection at peak load (P_{ult}), Δ_y is the mid-span deflection of the element at the yielding load; Δ_{uf} is the mid-span deflection at the ultimate failure state, *k* is the elastic stiffness which was equal slope of the initial linear part of the curve tan (*α*), and Ψ is the toughness specified as the area under the curve, ΔΨ, Δ*k*, and Δ*μ* is the increase ratios in toughness, stiffness and ductility index, respectively

from elastic to plastic behavior. The load–deflection curve rises until it reaches the peak load, representing the specimen's maximum capacity to resist the applied load. After reaching the peak load, the load gradually decreases as deflection increases. This stage is known as the softening stage, where the specimen experiences a reduction in load-carrying capacity and may exhibit a decrease in stiffness. The softening behavior is typically associated with the development of cracks, damage, or failure mechanisms within the specimen. The findings presented in Fig. 11 indicate that the implemented pre-stressed technique has significantly improved the load–deflection response of the tested specimens. The post-peak response, ultimate load, and deflection response were enhanced due to the proposed pre-stressed technique. The enhancement in the load–deflection curves proves that the proposed technique effectively increased the ductility and load-carrying capacity of the specimens.

3.2.1 First Crack and Ultimate Loads

The outcomes of the critical and ultimate stages are displayed in Table 5. Fig. 12 shows increasing ratios in the first crack and ultimate loads relative to the values of the unstrenghened control specimen (B_{C-L25}). The range of percentage increase values varied from a high of 144.87% for specimen B_7 to a minimum of 42.32% for specimen B_5. For all strengthened specimens, the first cracking load increased on average by as much as 101.05%, 80.15%, and 106.40% relative to the control specimen (B_{C-L25}) values for groups G_{II}, G_{III}, and G_{IV}, respectively. According to Fig. 12, the level of pre-stress in the bolts, the length of the strengthening plate, and the number of bolts play important roles in delaying the occurrence of the first crack in a prestressed system. Applying pre-stress to the bolts creates a compressive force within the beam, effectively redistributing the stresses and reducing tensile stresses at critical locations. This pre-compression increases the load-carrying capacity of the beam, allowing it to resist higher loads before reaching its cracking threshold. By reducing stress concentrations and enhancing load distribution, pre-stress helps delay crack initiation.

Similarly, the length of the strengthening plate influences load distribution and stress concentrations. A longer plate provides a larger area over which the loads can be distributed, reducing stress concentrations and minimizing the likelihood of crack initiation at specific locations. The increased stiffness resulting from a longer plate also limits the deflection of the beam under loading, further delaying crack initiation. Both factors, pre-stress, and plate length, contribute to improving the structural behavior and delaying the occurrence of the first crack in a prestressed system. By redistributing stresses, increasing load-carrying capacity, reducing stress concentrations, and enhancing stiffness, they collectively enhance the crack resistance and overall performance of the specimen.

The lowest percentage of increase in P_c was for specimen B_5, in which 2 pairs of bolts were utilized, and this ratio was increased to 124.9%, in which 4 pairs of bolts

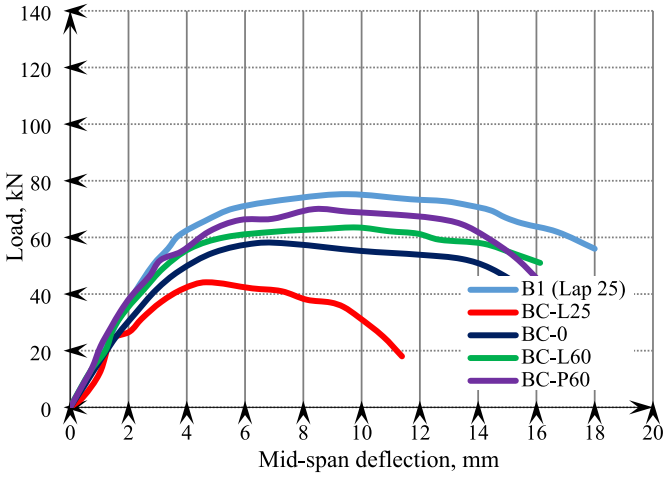

(a) Group G_I

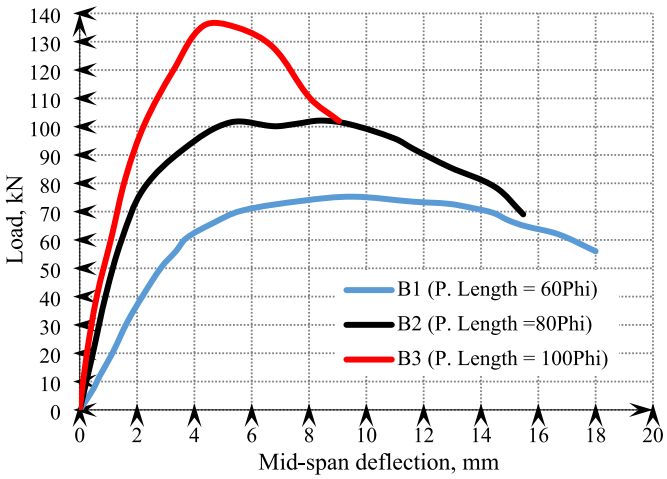

(b) Group G_{II}

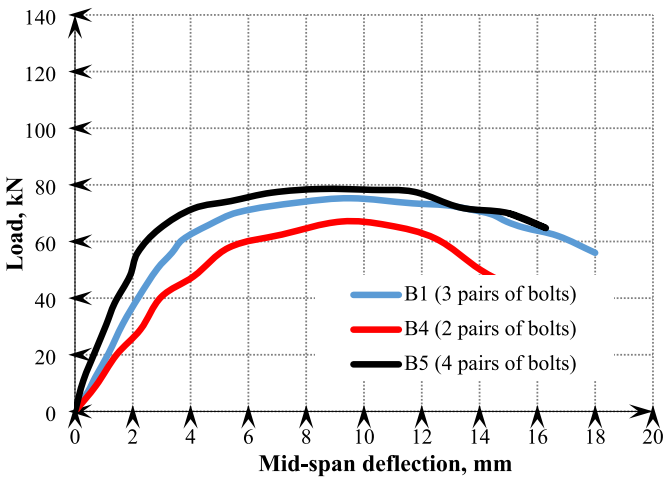

(c) Group G_{III}

Fig. 11 Load–deflection curves (mid-span deflection for all specimens)

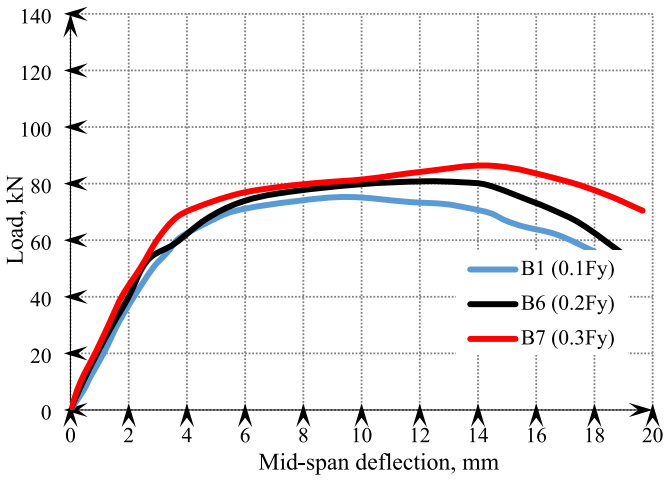

(d) Group G_{IV}

Fig. 11 continued

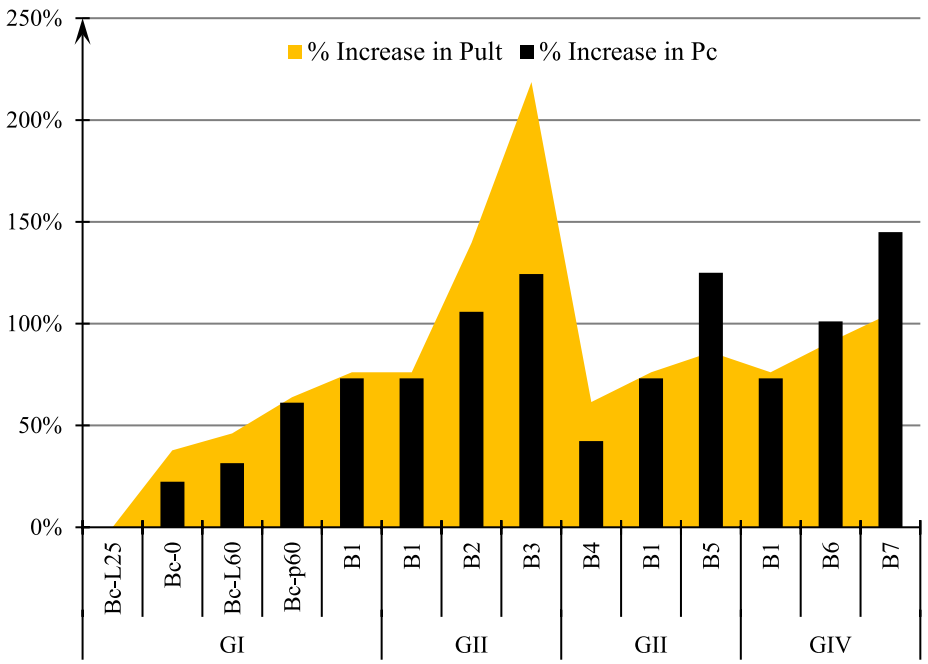

Fig. 12 Increase ratios in the first crack and ultimate loads of all specimens referenced to the control specimen ($B_{C\text{-}L25}$)

were utilized for the same plate length and prestressed level. This can be attributed to that a smaller bolt spacing helps to distribute the applied loads more evenly across the strengthening plate and the beam. This reduces stress concentrations, increases stiffness, prevents the occurrence of plate slippage, and lowers the likelihood of crack initiation at specific locations.

After the first crack, the cracks increased, and the contribution of concrete in resisting the applied loads reduced with the increase in the role of external prestressed strengening and internal steel in resisting the applied loads. According to Table 5, the ultimate load for the unstrengthened specimen (control specimen, $B_{C\text{-}L25}$) was recorded at a vertical load of 42.10 kN. By employing the proposed pre-stress method, the increase in the ultimate load (ΔP_{ult}) ranged between 61.52% and 218.65% compared to the control specimen $B_{C\text{-}L25}$. For group G_{II}, the average values of ΔP_{ult}

were recorded as 144.82%, compared to $B_{C\text{-}L25}$ (Fig. 12). In summary, the length of the strengthening bearing plate in the proposed pre-stress method affects the ultimate vertical load by improving load distribution, load transfer, reducing stress concentration, and enhancing the stiffness of the specimen. These factors collectively contribute to increasing the specimen's capacity to carry loads and withstand higher ultimate vertical loads. Group G_{III} (Fig. 12) gave values of ΔP_{ult} with a mean value of 74.53% with a range between 61.52% and 86.03% compared to $B_{C\text{-}L25}$. In general, increasing the number of pairs of bolts in the proposed pre-stress system has a slight increase in the ultimate load capacity of the beam. However, it is important to note that this parameter is particularly crucial for the first crack load rather than the ultimate load capacity. The bolts act as connectors, effectively joining different structural components together. By adding more bolts, the overall stiffness of the system increases, which can help resist deformation and distribute loads more evenly. However, it is worth noting that the primary purpose of the pre-stress system is to induce compressive forces in the concrete, which helps to counteract the tensile forces and prevent or delay crack formation. However, increasing the number of bolts alone may not significantly affect the magnitude of the compressive forces induced in the concrete. In the case of group G_{IV} (Fig. 12), the value of ΔP_{ult}, on average, the ultimate load capacity of the tested specimen was 90.73% higher compared to the reference specimen $B_{C\text{-}L25}$. The range of ΔP_{ult} values varied from 76.06% to 105.01%, indicating some variability in the performance of individual specimens within the group. Overall, the findings suggest that increasing the pre-stress levels in the bolts of the proposed pre-stress system had a positive impact on both the ultimate load capacity and the delay of first crack loads in the tested specimens. In general, these results demonstrate the effectiveness of the pre-stress system in enhancing the structural performance and load-carrying capacity of the specimens.

According to Table 1, which reviews previous research on the external strengthening of RC beams with tension lap splices using external methods, the range of insufficient lap length is 10 to 55 d_b, with a mean and median of 25 and 27 d_b, respectively. In the present study, the tension lap splice equals 25 d_b. The proposed pre-stress method for strengthening RC beams with tension lap splices is effective in significantly improving their strength. This improvement is demonstrated by comparing the maximum increase ratios of beam strength achieved through previous research methods and the present study. Fig. 13 shows that the maximum increase ratio obtained with the proposed prestress method is significantly higher than the ratios observed in previous research. This provides further evidence that the pre-stressing technique proposed here successfully increases the strength of RC beams that include insufficient tension lap splices.

3.2.2 Ultimate Final Deflection and Ductility

Ultimate final deflection (Δ_{uf}) is the deformation (mid-span) corresponding to 85% of the maximum force on the load–deflection curve's descending branch (Cohn & Bartlett, 1982; Mousavi et al., 2022). The peak deflection (Δ_p)

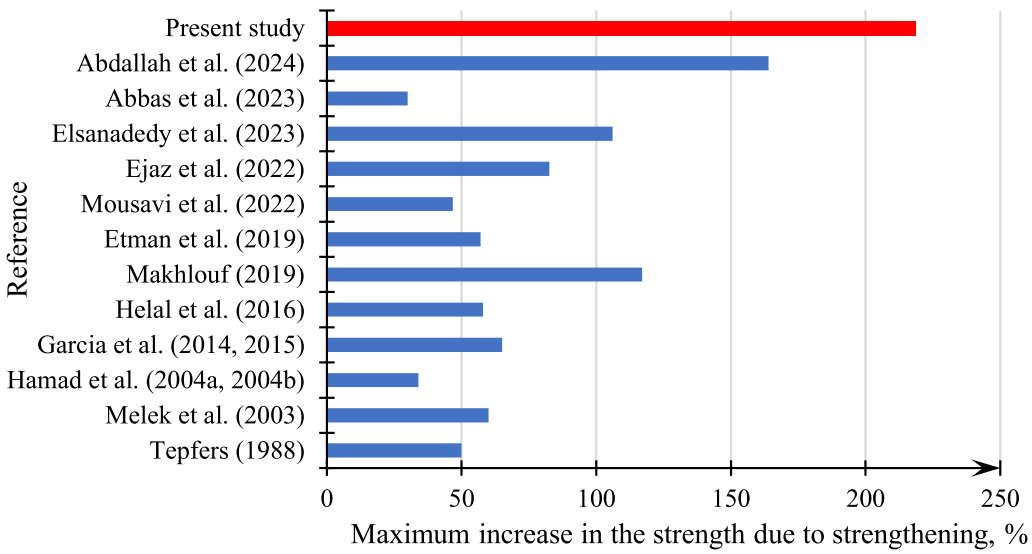

Fig. 13 Comparing the present study's and earlier research's improvements in the bending strength (4-point flexure load) due to external strengthening

is the deformation corresponding to the peak/ultimate load. Brittle failure caused by sudden fracture of the specimen should be avoided to assure large ultimate deformation (high enough ductility). According to Table 6, and Fig. 13 the Δ_p and Δ_{uf} for the unstrengthened lap spliced specimen (control specimen, $B_{C\text{-}L25}$) were 4.66 mm, and 7.95 mm, respectively. There was a significant improvement in the deformation behavior for all the strengthened specimens. The average values of the increase in Δ_p were recorded as 71.74%, 97 and 169.24% for G_{II}, G_{III}, and G_{IV}, respectively, with a mean value of 112.60% compared to specimen $B_{C\text{-}L25}$ (Fig. 14). In addition, on average, the increase in Δ_{uf} was 62.26% for G_{II}, 95.00% for G_{III}, and 120.12% for G_{IV}, with a mean value of 97.33% when compared to specimen $B_{C\text{-}L25}$.

The determination of ductility and flexural toughness can be achieved by analyzing flexural load–deflection curves. Ductility is measured by analyzing the deflection in the post-peak phase, whereas flexural toughness is computed as the area under the whole load–deflection curve (Low & Beaudoin, 1994). The ductility analysis of the strengthened beams involves the calculation of two ductility indices: the peak deflection ductility index (μ_p) and the ultimate deflection ductility index (μ_{uf}). These indices are derived from three key deflection values: the yield deflection (Δ_y), the peak deflection (Δ_p), and the ultimate deflection (Δ_{uf}). The purpose of this analysis is to assess the effect of the proposed pre-stressed technique on the ductility of the strengthened beams. The findings of this analysis are displayed in Table 6 and Fig. 14. The peak deflection ductility index (μ_p) is determined by dividing the peak deflection (Δ_p) by the yield deflection (Δ_y) (Yoo et al., 2017; Abbas et al. 2019). This index provides a measure of the ability of the beams to undergo significant deflection beyond the yielding point. A higher μp value indicates greater ductility, as the beams can sustain larger deformations before failure. The ultimate deflection ductility index (μ_{uf}) is calculated by dividing the ultimate deflection (Δ_{uf}) by the yield deflection (Δ_y) (Abbas et al., 2019; Elrakib, 2013; Hasgul et al., 2018; Yang et al., 2010; Yoo & Moon, 2018; Yoo et al., 2017). This index quantifies the ability of the beams to sustain deflection beyond the peak load and into the post-peak phase. A higher μ_{uf} value indicates a higher capacity of the beams to undergo large deformations and absorb energy before failure. In general, the results presented in Table 6 and Fig. 14 show that the proposed strengthening technique significantly enhanced the strengthened beams' ductility. The increase in the ductility index ranged between 69.3% and 175%, with a mean value of 94% relative to the control specimen $B_{C\text{-}L25}$. The deflection ductility indices, $\mu_{p,}$ and μ_{uf} of strengthened RC beams were higher than non-strengthened specimens. In the present study, the increase in μ_{uf} ($\Delta\mu_{uf}$) ranged between 10.58% and 175%, with a mean value of 94% relative to the control specimen $B_{C\text{-}L25}$. In comparison with the control specimen $B_{C\text{-}L25}$, the values of $\Delta\mu_p$ varied from 17.77% to 173.08%, averaging 120.16%. However, the ultimate deflection ductility index (μ_{uf}) considers the sustained load-carrying capacity of the beams beyond the peak load (at least 85% beyond the peak load), preventing sudden brittle failure and enhancing their structural integrity (Elrakib, 2013;

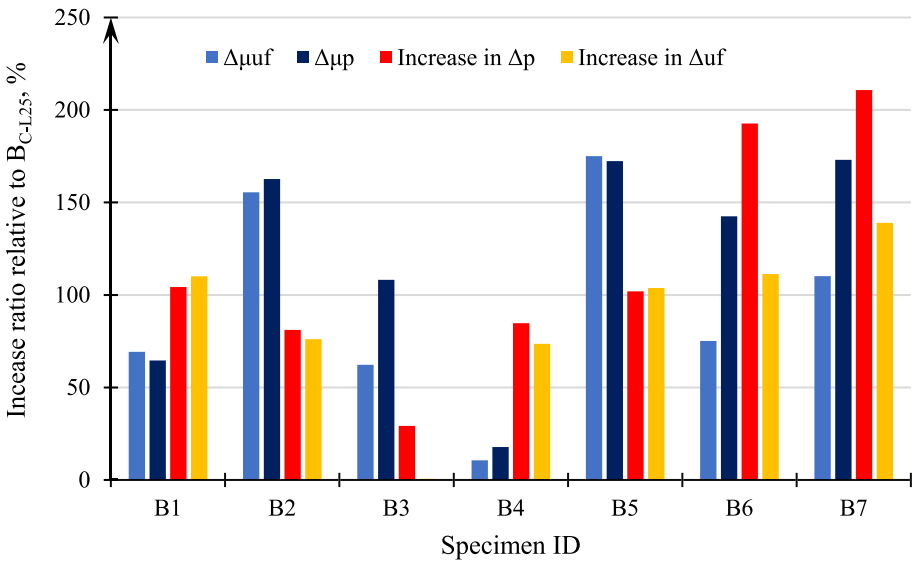

Fig. 14 Increase ratios in the ultimate final deflection (Δ_{uf}), peak deflection (Δ_p), peak deflection ductility index (μ_p), and ultimate deflection ductility index (μ_{uf})

Shin et al., 1989). The average values of $\Delta\mu_{uf}$ were 95.66%, 84.96%, and 84.87% for G_{II}, G_{III}, and G_{VI}, respectively, compared to specimen $B_{C\text{-}L25}$. Specimen B_4, which had 2 pairs of bolts, had the lowest improvement in the deflection ductility index, with a value of 10.58% for μ_{uf} and 17.77% for $\Delta\mu_p$.

3.2.3 Elastic Stiffness (k)

The resistance of a beam to initial deformation is mostly related to its elastic stiffness, but its ability to absorb energy before failure is represented by its flexure toughness, which is measured during bending. Elastic stiffness (k) is the curve's initial slope (the linear part). Table 6 and Fig. 15 show a considerable increase in elastic stiffness (k) for all the strengthened specimens. The range of increase in elastic stiffness (Δk) varies, with the lowest value being 23.97% (in specimen B_4 with two pairs of bolts) and the highest value being 322.22% (in specimen B_3 with a plate length of 1000 mm) compared to the control specimen $B_{C\text{-}L25}$. In comparison with specimen $B_{C\text{-}L25}$, the average values of Δk for G_{II}, G_{III}, and G_{IV} were 200.80%, 60.47%, and 63.80%, respectively, with an average of 101.35%. Overall, the increased elastic stiffness in the strengthened specimens improves their structural performance by enhancing rigidity, load distribution, crack resistance, and serviceability. These benefits contribute to a more robust and reliable structure that can withstand applied loads more effectively. This proves that the pre-stress strengthening technique employed in the paper was beneficial and effective.

3.2.4 Flexural Toughness (ψ)

As an indication of the specimens' capacity to withstand the formation of cracks, toughness has been proposed as a metric for assessing deformability (or fast fracture) (Smart & Jensen, 1997). In this study, flexural toughness (Ψ) is defined as the area under the load–deflection curve. Notably, all curves were finished at 0.8 f_{bu} after the peak.

As presented in Table 6 and Fig. 16, the flexural toughness (Ψ) of the control specimen $B_{C\text{-}L25}$ was measured to be 350 kN.mm. However, for all the strengthened specimens, there was a notable increase in flexural toughness ($\Delta\Psi$). The increase in flexural toughness ranged between 101.43% and 308.57%, with an average increase of 205% compared to the control specimen $B_{C\text{-}L25}$. Specifically, the average increase in flexural toughness ($\Delta\Psi$) was found to be 202.76%, 170%, and 248% for the G_{II}, G_{III}, and G_{IV} strengthened specimens, respectively, when compared to specimen $B_{C\text{-}L25}$. These findings suggest that the proposed strengthening method successfully enhanced the deformability and crack resistance of the specimens. The reinforced specimens exhibited significantly higher flexural toughness values, indicating their improved ability to withstand crack growth and resist fast fracture compared to the control specimen.

3.3 Applicability and Future Outlook

The classification of this technique as a prestressing method is based on the principle that applying compressive forces through the bolts alters the internal stress distribution within the beam. The compressive forces exerted through the bolts translate into pressure under the reinforcement plates, delaying crack

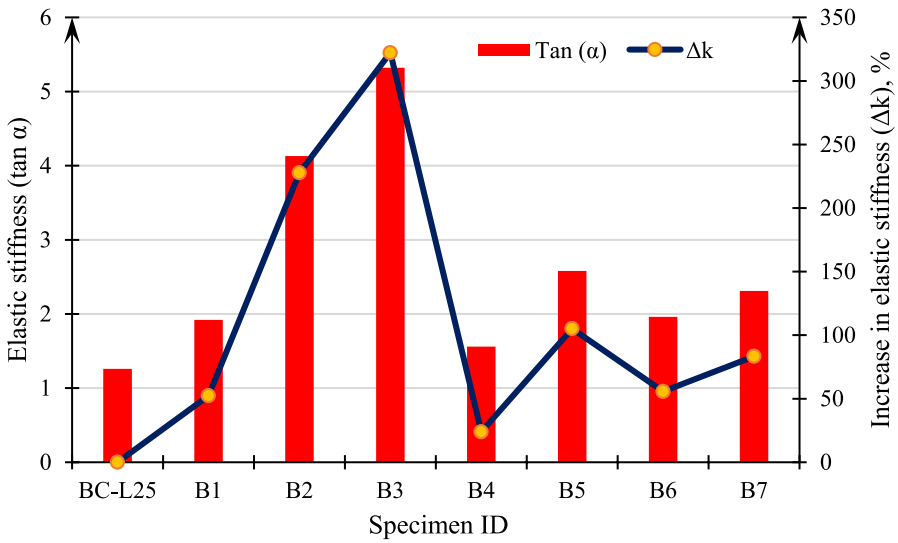

Fig. 15 Elastic stiffness and the ratios of its increases relative to $B_{C\text{-}L25}$

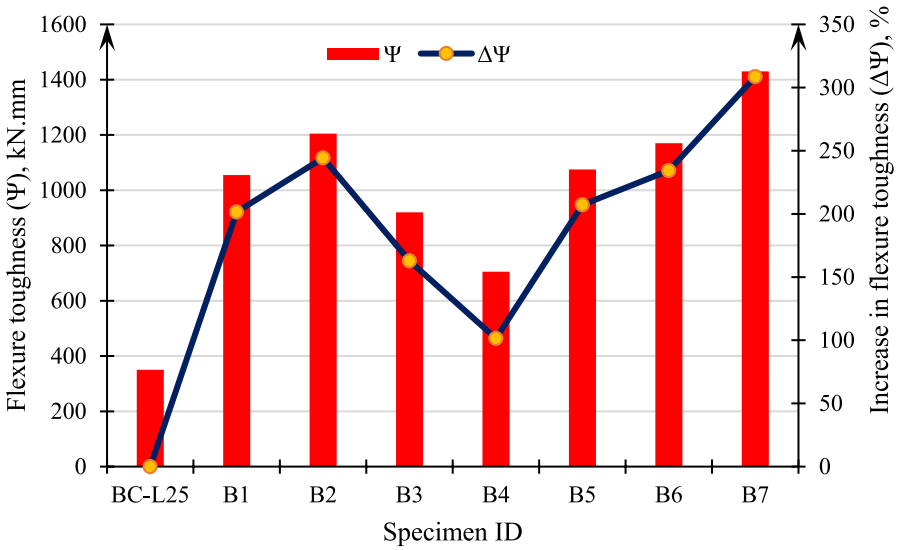

Fig. 16 Flexure toughness and the ratios of its increases relative to $B_{C\text{-}L25}$

formation and increasing the overall resistance of the section. The methodology successfully demonstrates the ability to induce significant prestressing in the beams, which is a fundamental characteristic of pre-stressing techniques.

The proposed pre-stressing technique presents several advantages over traditional strengthening methods, such as externally bonded (EB) or near-surface-mounted (NSM) systems. Unlike traditional methods that often rely on adhesive materials and hydraulic jacks, this technique utilizes bolts, load-transferring brackets, and bearing plates, allowing for a faster and more straightforward application process. This is particularly advantageous in situations, where time-sensitive repairs are necessary. The ease of implementation enhances the technique's practicality for engineers and contractors, making it a viable alternative for enhancing structural integrity.

The study yielded promising results, demonstrating significant enhancements in various performance metrics of the strengthened beams. The ultimate load capacities increased by 61.52–218.65%, and first cracking loads improved by 80.15–106.40% compared to control specimens. In addition, the strengthened beams showed notable improvements in elastic stiffness and flexural toughness, with average increases of 205.5% and 101.35%, respectively. These results indicate that the pre-stressing technique not only increases load-carrying capacity but also enhances ductility and crack resistance, contributing to overall structural resilience.

Looking ahead, the future outlook for this pre-stressing technique is promising. Ongoing research will focus on further optimizing the method through parametric studies to explore different configurations and materials. Establishing comprehensive guidelines for implementation will enhance its applicability across various structural scenarios. As the construction industry increasingly prioritizes efficiency and sustainability, this technique could play a crucial role in modern reinforcement practices, offering a robust alternative to traditional methods. Continued validation through field studies and long-term performance assessments will be essential to solidify its standing as a reliable solution for reinforced concrete strengthening.

4 Conclusion

The paper aims to strengthen RC beams with substandard tension lap splices using a novel pre-stressing method. To evaluate the effectiveness of the proposed method, a series of experimental tests were conducted using eleven test specimens with dimensions $100\times200\times1500$ mm^3. The investigation considered three main variables for eight strengthened specimens: the length of the strengthening plate ($L_s=60d_b$, $80d_b$, and $100d_b$), the number of bolts ($N_b=2$, 3, and 4 pairs), and the pre-stress level in the bolts (PL = 0.1*fy*, 0.2*fy*, and $0.3f_y$). The effects of the proposed strengthening technique on ultimate load (P_{ult}), first cracking load (Pc), deformation behavior, failure pattern, cracks distribution, deflection ductility, flexure toughness, and elastic stiffness were investigated. Based on the results and analyses of this research, the following conclusions are drawn:

1) Insufficient lap splice length resulted in slippage of tension rebars and limited, wide flexural cracks near

the end of the lap zone. The results show that the proposed pre-stressed technique affects positively the load-carrying capacity, the beams' crack pattern, and the failure conditions. The increased length of the bearing plate in specimens B2 and B3 resulted in more distributed cracks along the span of the beam compared to other specimens.

2) The strengthened specimens showed a substantial increase in both peak deflection (Δ_p) and ultimate final deflection (Δ_{uf}) compared to the control specimen ($B_{C\text{-}L25}$). The average increase in Δ_p for the strengthened specimens was 112.60%, while the average increase in Δ_{uf} was 97.33%, demonstrating the effectiveness of the strengthening technique.
3) The proposed pre-stress technique significantly increased both the first crack and ultimate loads of the strengthened specimens compared to the control specimen. The first crack load increased by an average of 80.15–106.40% for different groups of strengthened specimens. Similarly, the ultimate load showed an increase ranging from 61.52% to 218.65% compared to the control specimen.
4) The ductility of the strengthened RC beams was greatly enhanced by the proposed strengthening method. In comparison with the control specimen $B_{C\text{-}L25}$, the values of the increase in peak deflection ductility index (μ_p) varied from 17.77% to 173.08%, averaging 120.16%, while the increase in the ultimate deflection ductility index (μuf) ranged between 10.58% and 175%, and averaging 94%.
5) The strengthened specimens exhibited a notable increase in flexural toughness, ranging from 101.43% to 308.57%, with an average increase of 205% compared to the control specimen. This improvement signifies enhanced deformability, increased crack resistance, and improved ability to withstand crack growth and resist fast fracture.
6) The range of increase in elastic stiffness (Δk) varies, with the lowest value being 23.97% (in specimen B4 with two pairs of bolts) and the highest value being 322.22% (in specimen B3 with a plate length of 1000 mm) compared to the control specimen BC-L25.

Acknowledgements
The authors acknowledge the contributions of technical staff at reinforced concrete laboratory, faculty of engineering, Kafrelsheikh University, Egypt, for providing great assistance and helpful comments in executing the experimental program.

Author Contributions
Mohamed Hamed Zakaria and Boshra Eltaly led the conceptualization, funding acquisition, investigation, project administration, resources, supervision, validation, and writing. Ahmed Elkhouly contributed to supervision, validation, and manuscript review. Roba Osman, a master's student, contributed to data collection, investigation, and initial drafting under supervision. All authors read and approved the final manuscript.

Funding
Open access funding provided by The Science, Technology & Innovation Funding Authority (STDF) in cooperation with The Egyptian Knowledge Bank (EKB).

Availability of Data and Materials
The experimental data can be obtained through email communication with the author at boushra_eltaly@yahoo.com.

Declarations

Ethics Approval and Consent to Participate
Not applicable.

Consent for Publication
All authors agreed to publish.

Competing Interests
Not applicable.

Author details
[1]Faculty of Engineering, Menoufia University, Shebeen Elkom, Egypt. [2]Faculty of Engineering, Kafrelsheikh University, Kafr El-Shaikh, Egypt.

Received: 24 June 2024 Accepted: 15 February 2025
Published: 9 June 2025

References

Abbas, H., Elsanadedy, H., Alaoud, L., Almusallam, T., & Al-Salloum, Y. (2023). Effect of confining stirrups and bar gap in improving bond behavior of glass fiber reinforced polymer (GFRP) bar lap splices in RC beams. *Construction and Building Materials, 365*, 129943. https://doi.org/10.1016/j.conbuildmat.2022.129943

Abbass, A., Abid, S., & Özakça, M. (2019). Experimental investigation on the effect of steel fibers on the flexural behavior and ductility of high-strength concrete hollow beams. *Advances in Civil Engineering*. https://doi.org/10.1155/2019/8390345

Abdallah, A. M., Badawi, M., Elsamak, G., Hu, J. W., Mlybari, E. A., & Ghalla, M. (2024). Strengthening of RC beams with inadequate lap splice length using cast-in-situ and anchored precast ECC ferrocement layers mitigating construction failure risk. *Case Studies in Construction Materials, 20*, e02747. https://doi.org/10.1016/j.cscm.2023.e02747

Abdalla, J. A., Mohammed, A., & Hawileh, R. A. (2020). Flexural strengthening of reinforced concrete beams with externally bonded hybrid systems. *Procedia Structural Integrity, 28*, 2312–2319. https://doi.org/10.1016/j.prostr.2020.11.078

ACI 440.2R-02. (2002). Guide for the design and construction of externally bonded FRP systems for strengthening concrete structures. Farmington Hills, MI: American.

ACI Committee 408. (2003). ACI 408R-03 bond and development of straight reinforcing bars in tension. American Concrete Institute.

ACI (318-19) Committee. (2019). Building Code Requirement for Structural Concrete and Commentary. Reported by American Concrete Institute Committee. American Concrete Institute: Farmington Hills, MI, USA. Materials-Online/ACI_318-Building-Code-2011.

Akın, S. K., Kartal, S., Müsevitoğlu, A., Sancıoğlu, S., Zia, A. J., & Ilgün, A. (2022). Macro and micro polypropylene fiber effect on reinforced concrete beams with insufficient lap splice length. *Case Studies in Construction Materials, 16*, e01005. https://doi.org/10.1016/j.cscm.2022.e01005

Albuja-Sánchez, J., Damián-Chalán, A., & Escobar, D. (2024). Experimental studies and application of fiber-reinforced polymers (FRPs) in civil infrastructure systems: A state-of-the-art review. *Polymers, 16*(2), 250. https://doi.org/10.3390/polym16020250

Alexander, M. G., Beushausen, H. D., Dehn, F., & Moyo, P. (Eds.). (2008). Concrete repair, rehabilitation and retrofitting II: 2nd International Conference on

Concrete Repair, Rehabilitation and Retrofitting, ICCRRR-2, 24–26 November 2008, Cape Town, South Africa. CRC Press. (2008). https://doi.org/10.1201/9781439828403

Alharbi, Y. R., Galal, M., Abadel, A. A., & Kohail, M. (2021). Bond behavior between concrete and steel rebars for stressed elements. *Ain Shams Engineering Journal, 12*(2), 1231–1239. https://doi.org/10.1016/j.asej.2020.10.001

Almeida, J. P., Prodan, O., Tarquini, D., & Beyer, K. (2017). Influence of lap splices on the deformation capacity of RC walls. I: Database assembly, recent experimental data, and findings for model development. *Journal of Structural Engineering, 143*(12), 04017156. https://doi.org/10.1061/(ASCE)ST.1943-541X.0001853

Al-Quraishi, H., Al-Farttoosi, M., & AbdulKhudhur, R. (2019). Tension lap splice length of reinforcing bars embedded in reactive powder concrete (RPC). *Structures, 19*, 362–368. https://doi.org/10.1016/j.istruc.2018.12.011

Aslam, M., Shafigh, P., Jumaat, M. Z., & Shah, S. N. R. (2015). Strengthening of RC beams using pre-stressed fiber reinforced polymers—A review. *Construction and Building Materials, 82*, 235–256. https://doi.org/10.1016/j.conbuildmat.2015.02.051

Assaad, F., Hany, N., Fawaz, G., Hantouche, E., & Harajli, M. (2021). Effect of active and passive concrete confinement on the bond stress-slip response of steel bars in tension. *Construction and Building Materials, 305*, 124737. https://doi.org/10.1016/j.conbuildmat.2021.124737

ASTM C – 881 (American Society of Testing and Material). (2008). Standard Specification for Epoxy-Resin-Base Bonding Systems for Concrete. West Conshohocken, PA.

Bhattacharjee, J. (2016). Repair, rehabilitation & retrofitting of RCC for sustainable development with case studies. *Civil Engineering and Urban Planning: An International Journal (CiVEJ), 3*, 33–47. https://doi.org/10.5121/CIVEJ.2016.3203

Bournas, D. A., & Triantafillou, T. C. (2011). Bond strength of lap-spliced bars in concrete confined with composite jackets. *Journal of Composites for Construction, 15*(2), 156–167. https://doi.org/10.1061/(ASCE)CC.1943-5614.0000078

Bousias, S., Spathis, A. L., & Fardis, M. N. (2007). Seismic retrofitting of columns with lap spliced smooth bars through FRP or concrete jackets. *Journal of Earthquake Engineering, 11*(5), 653–674. https://doi.org/10.1080/13632460601125714

Breña, S. F., & Schlick, B. M. (2007). Hysteretic behavior of bridge columns with FRP-jacketed lap splices designed for moderate ductility enhancement. *Journal of Composites for Construction, 11*(6), 565–574. https://doi.org/10.1061/(ASCE)1090-0268(2007)11:6(565)

BS EN 12004-2. (2017). Adhesives for ceramic tiles. Test methods, European Standard specifies the methods for determining characteristics for adhesives used in internal and external installation of ceramic tiles.

BS12. (1978). Ordinary and rapid hardening Portland cement. British standard institution, London.

Chen, G. M., Teng, J. G., & Chen, J. F. (2011). Finite-element modeling of intermediate crack debonding in FRP-plated RC beams. *Journal of Composites for Construction, 15*(3), 339–353. https://doi.org/10.1061/(ASCE)CC.1943-5614.0000157

Chen, G. M., Teng, J. G., Chen, J. F., & Xiao, Q. G. (2015). Finite element modeling of debonding failures in FRP-strengthened RC beams: A dynamic approach. *Computers & Structures, 158*, 167–183. https://doi.org/10.1016/j.compstruc.2015.05.023

Cohn, M. Z., & Bartlett, M. (1982). Computer-simulated flexural tests of partially prestressed concrete sections. *Journal of the Structural Division, 108*(12), 2747–2765. https://doi.org/10.1061/(ASCE)0733-9445(1983)109:11(275

Croppi, J. I., Ahrens, M. A., Palmeri, A., Piccinin, R., & Mark, P. (2024). Experimental investigation on post-installed lap splices in ordinary and steel fiber-reinforced concrete. *Materials and Structures, 57*(8), 180. https://doi.org/10.1617/s11527-024-02450-7

CSA (Canadian Standards Association). (2002). *Design and construction of building components with fibre-reinforced polymers* (No. 2). Canadian Standards Association. http://worldcat.org/isbn/0080439454

Dabiri, H., Kheyroddin, A., & Dall'Asta, A. (2022). Splice methods used for reinforcement steel bars: A state-of-the-art review. *Construction and Building Materials, 320*, 126198. https://doi.org/10.1016/j.conbuildmat.2021.126198

Dagenais, M. A., & Massicotte, B. (2015). Tension lap splices strengthened with ultrahigh-performance fiber-reinforced concrete. *Journal of Materials in Civil Engineering, 27*(7), 04014206. https://doi.org/10.1061/(ASCE)MT.1943-5533.0001169

De Lorenzis, L., & Teng, J. G. (2007). Near-surface mounted FRP reinforcement: An emerging technique for strengthening structures. *Composites Part B: Engineering, 38*(2), 119–143. https://doi.org/10.1016/j.compositesb.2006.08.003

E.C.P. 203-2018. (2018). Egyptian code for design and construction of reinforced concrete structures. Housing and Building National Research Center. Ministry of Housing, Utilities and Urban Planning, Cairo.

Ejaz, A., Ruangrassamee, A., Kruavit, P., Udomworarat, P., & Wijeyewickrema, A. C. (2022). Strengthening of substandard lap splices using hollow steel section (HSS) collars. *Structures, 46*, 128–145. https://doi.org/10.1016/j.istruc.2022.10.030

El-Hacha, R., & Gaafar, M. (2011). Flexural strengthening of reinforced concrete beams using prestressed, near-surface-mounted CFRP bars. *PCI Journal, 56*(4), 134–151. https://doi.org/10.15554/pcij.09012011.134.151

Elrakib, T. M. (2013). Performance evaluation of HSC beams with low flexural reinforcement. *HBRC Journal, 9*(1), 49–59. https://doi.org/10.1016/j.hbrcj.2012.12.006

Elsanadedy, H., Alaoud, L., Abbas, H., Almusallam, T., & Al-Salloum, Y. (2023). Externally bonded CFRP composites versus steel stirrups for the confinement of substandard lap spliced GFRP bars in RC beams. *Composite Structures, 306*, 116602. https://doi.org/10.1016/j.compstruct.2022.116602

Etman, E., Atta, A., Baraghith, A., & Edris, A. (2019). Efficient steel reinforced UHP SHCC strengthening for lap spliced RC Beams. *International Journal of Advances in Structural and Geotechnical Engineering*. https://doi.org/10.21608/asge.2019.254653

Fayed, S., Mansour, W., Tawfik, T. A., Sabol, P., & Katunský, D. (2023). Techniques used for bond strengthening of sub-standard splices in concrete: A review study. *Processes, 11*(4), 1119. https://doi.org/10.1016/j.cscm.2022.e01532

Foraboschi, P. (2022). Strengthening of reinforced concrete beams subjected to concentrated loads using externally bonded fiber composite materials. *Materials, 15*(6), 2328. https://doi.org/10.20944/preprints202201.0041.v1

Garcia, R., Helal, Y., Pilakoutas, K., & Guadagnini, M. (2014). Bond behaviour of substandard splices in RC beams externally confined with CFRP. *Construction and Building Materials, 50*, 340–351. https://doi.org/10.1016/j.conbuildmat.2013.09.021

Garcia, R., Helal, Y., Pilakoutas, K., & Guadagnini, M. (2015). Bond strength of short lap splices in RC beams confined with steel stirrups or external CFRP. *Materials and Structures, 48*, 277–293. https://doi.org/10.1617/s11527-013-0183-5

Gillani, A. S. M., Lee, S. G., Lee, S. H., Lee, H., & Hong, K. J. (2021). Local behavior of lap-spliced deformed rebars in reinforced concrete beams. *Materials, 14*(23), 7186. https://doi.org/10.3390/ma14237186

Haefliger, S., Kaufmann, W., & Thoma, K. (2022). Modelling the load-deformation behaviour of lap splices with the Tension Chord Model. *Engineering Structures, 252*, 113606. https://doi.org/10.1016/j.engstruct.2021.113606

Hamad, B. S., Rteil, A. A., Salwan, B. R., & Soudki, K. A. (2004b). Behavior of bond-critical regions wrapped with fiber-reinforced polymer sheets in normal and high-strength concrete. *Journal of Composites for Construction, 8*(3), 248–257. https://doi.org/10.1061/(ASCE)1090-0268(2004)8:3(248)

Hamad, B. S., Rteil, A. A., & Soudki, K. A. (2004a). Bond strength of tension lap splices in high-strength concrete beams strengthened with glass fiber reinforced polymer wraps. *Journal of Composites for Construction, 8*(1), 14–21. https://doi.org/10.1061/(ASCE)1090-0268(2004)8:1(14)

Harajli, M. H. (2009). Bond strengthening of lap spliced reinforcement using external FRP jackets: An effective technique for seismic retrofit of rectangular or circular RC columns. *Construction and Building Materials, 23*(3), 1265–1278. https://doi.org/10.1016/j.conbuildmat.2008.07.028

Hasan, G. N., Das, C. H. O. T. O. N., & Sumon, S. M. F. H. (2015). *Splice length of reinforcing bars calculated in different design codes* (Doctoral dissertation, Ahsanullah University of Science and Technology). https://www.academia.edu/19890554/splice_length_of_reinforcing_bars_calculated_in_different_design_codes

Hasgul, U., Turker, K., Birol, T., & Yavas, A. (2018). Flexural behavior of ultra-high-performance fiber reinforced concrete beams with low and high reinforcement ratios. *Structural Concrete, 19*(6), 1577–1590. https://doi.org/10.1002/suco.201700089

Helal, Y., Garcia, R., Pilakoutas, K., Guadagnini, M., & Hajirasouliha, I. (2016). Strengthening of short splices in RC beams using Post-Tensioned Metal

Straps. *Materials and Structures, 49*, 133–147. https://doi.org/10.1617/s11527-013-0183-5
Hussein, M., Afefy, H. M., & Khalil, A.-H.A.-K. (2013). Innovative repair technique for RC beams predamaged in Shear. *Journal of Composites for Construction*. https://doi.org/10.1061/(asce)cc.1943-5614.0000404
Kadhim, M. M., Jawdhari, A., & Peiris, A. (2021). Evaluation of lap-splices in NSM FRP rods for retrofitting RC members. *Structures, 30*, 877–894. https://doi.org/10.1016/j.istruc.2021.01.054
Karayannis, C. G., Chalioris, C. E., & Sirkelis, G. M. (2008). Local retrofit of exterior RC beam–column joints using thin RC jackets—An experimental study. *Earthquake Engineering & Structural Dynamics, 37*(5), 727–746. https://doi.org/10.1002/eqe.783
Karkarna, Y. M., Bahadori-Jahromi, A., Jahromi, H. Z., & Halliwell, E. (2023). An investigation into the tension lap splices. *Engineering Future Sustainability*. https://doi.org/10.36828/efs.229
Low, N. M., & Beaudoin, J. J. (1994). The flexural toughness and ductility of portland cement-based binders reinforced with wollastonite micro-fibres. *Cement and Concrete Research, 24*(2), 250–258. https://doi.org/10.1016/0008-8846(94)90050-7
Mabrouk, R. T., & Mounir, A. (2018). Behavior of RC beams with tension lap splices confined with transverse reinforcement using different types of concrete under pure bending. *Alexandria Engineering Journal, 57*(3), 1727–1740. https://doi.org/10.1016/j.aej.2017.05.001
Makhlouf, M. H. (2019). Effectiveness of various techniques using FRP for the strengthening of RC beams with tension lap splices. *Journal of Engineering Research and Reports, 6*(1), 1–18. https://doi.org/10.9734/jerr/2019/v6i116937
Maruyama, K. (2001). Recommendations for upgrading of concrete structures with use of continuous fiber sheets. (CRID: 1130282269913432576 – ISBN: 4810603555).
Masud, M., Chen, H., Sawab, J., Huang, H. W., Xu, B., Mo, Y. L., & Hsu, T. T. (2020). Performance of non-contact lap splices in geometrically dissimilar bridge column to drilled shaft connections. *Engineering Structures, 209*, 110000. https://doi.org/10.1016/j.engstruct.2019.110000
Melek, M., Conte, J. P., & Wallace, J. W. (2003). *Experimental assessment of columns with short lap splices subjected to cyclic loads*. Pacific Earthquake Engineering Research Center.
Meng, X., Gao, J., Xu, T., Cai, T., Wu, Z., Gao, K., et al. (2023). Experimental investigation on realistic model for local bond stress-slip relationship between ribbed GFRP bars and concrete. *Advances in Structural Engineering*. https://doi.org/10.1177/13694332231184319
Metelli, G., Cairns, J., & Plizzari, G. (2015). The influence of percentage of bars lapped on performance of splices. *Materials and Structures, 48*, 2983–2996. https://doi.org/10.1617/s11527-014-0371-y
Mousavi, S. R., Sohrabi, M. R., Moodi, Y., & Gholamhosseini, E. (2022). Strengthening of lap-spliced RC beams using near-surface mounting method. *Iranian Journal of Science and Technology, Transactions of Civil Engineering*. https://doi.org/10.1007/s40996-020-00577-5
Najafgholipour, M. A., Dehghan, S. M., Khani, M., & Heidari, A. (2018). The performance of lap splices in RC beams under inelastic reversed cyclic loading. *Structures, 15*, 279–291. https://doi.org/10.1139/l86-103
Naser, M. Z., Hawileh, R. A., & Abdalla, J. A. (2019). Fiber-reinforced polymer composites in strengthening reinforced concrete structures: A critical review. *Engineering Structures, 198*, 109542. https://doi.org/10.1016/j.engstruct.2019.109542
Oehlers, D. J., Muhamad, R., & Ali, M. M. (2013). Serviceability flexural ductility of FRP RC beams: A discrete rotation approach. *Construction and Building Materials, 49*, 974–984. https://doi.org/10.1016/j.conbuildmat.2012.10.001
Rezazadeh, M., Costa, I., & Barros, J. (2014). Influence of prestress level on NSM CFRP laminates for the flexural strengthening of RC Beams. *Composite Structures, 116*, 489–500. https://doi.org/10.1016/j.compstruct.2014.05.043
Salmi, A. (2024). Prediction of the bond strength of externally bonded FRP sheets applied to concrete via grooves technique using artificial neural networks. *Journal of Composites Science, 8*(1), 30. https://doi.org/10.3390/jcs8010030
Seręga, S., & Faustmann, D. H. (2022). Flexural strengthening of reinforced concrete beams using external tendons. *Engineering Structures, 252*, 113277. https://doi.org/10.1016/j.engstruct.2021.113277
Shin, S. W., Ghosh, S. K., & Moreno, J. (1989). Flexural ductility of ultra-high-strength concrete members. *Structural Journal, 86*(4), 394–400. https://doi.org/10.14359/2877
Siddika, A., Al Mamun, M. A., Ferdous, W., & Alyousef, R. (2020). Performances, challenges and opportunities in strengthening reinforced concrete structures by using FRPs—A state-of-the-art review. *Engineering Failure Analysis, 111*, 104480. https://doi.org/10.1016/j.engfailanal.2020.104480
Slaitas, J. (2024). Universal bond models of FRP reinforcements externally bonded and near-surface mounted to RC elements in bending. *Materials, 17*(2), 493. https://doi.org/10.3390/ma17020493
Smart, C. W., & Jensen, D. W. (1997). Flexure of concrete beams reinforced with advanced composite orthogrids. *Journal of Aerospace Engineering, 10*(1), 7–15. https://doi.org/10.1061/(ASCE)0893-1321(1997)10:1(7)
Smith, S. T., & Teng, J. G. (2002). FRP-strengthened RC beams. II: Assessment of debonding strength models. *Engineering Structures, 24*(4), 397–417. https://doi.org/10.1016/S0141-0296(01)00106-7
Subramaniam, K. V., Ali-Ahmad, M., & Ghosn, M. (2008). Freeze–thaw degradation of FRP–concrete interface: Impact on cohesive fracture response. *Engineering Fracture Mechanics, 75*(13), 3924–3940. https://doi.org/10.1016/j.engfracmech.2007.12.016
Taie, B., Mandor, A., & El Refai, A. (2024). Experimental and numerical investigation of two–span RC beams strengthened with fiber–reinforced cementitious matrix (FRCM). *Engineering Structures, 300*, 117246. https://doi.org/10.1016/j.engstruct.2023.117246
Tarabia, A. M., Mahmoud, Z. I., Shoukry, M. S., & Abudina, A. A. (2016). Performance of RC slabs with lap splices using headed bars. *Alexandria Engineering Journal, 55*(3), 2729–2740. https://doi.org/10.1016/j.aej.2016.05.018
Teguh, M., & Mahlisani, N. (2016). Experimental study on flexural behavior of reinforced concrete beams with variety lap splices of reinforcing steel bars. *Applied Mechanics and Materials, 845*, 132–139. https://doi.org/10.4028/www.scientific.net/amm.845.132
Teng, J. G., Smith, S. T., Yao, J., & Chen, J. F. (2003). Intermediate crack-induced debonding in RC beams and slabs. *Construction and Building Materials, 17*(6–7), 447–462. https://doi.org/10.1016/S0950-0618(03)00043-6
Tepfers, R. (1988). Overlap splices for ribbed bars for free use in a concrete structure. *Nordic Concrete Research, 7*, 273–283.
Verderame, G. M., Fabbrocino, G., & Manfredi, G. (2008). Seismic response of rc columns with smooth reinforcement Part i: Monotonic Tests. *Engineering Structures, 30*(9), 2277–2288. https://doi.org/10.1016/j.engstruct.2008.01.025
Wang, W. W., Dai, J. G., & Harries, K. A. (2013). Intermediate crack-induced debonding in RC beams externally strengthened with pre-stressed FRP laminates. *Journal of Reinforced Plastics and Composites, 32*(23), 1842–1857. https://doi.org/10.1016/S0950-0618(03)00043-6
Wang, W. W., Dai, J. G., Harries, K. A., & Bao, Q. H. (2012). Pre-stress losses and flexural behavior of reinforced concrete beams strengthened with posttensioned CFRP sheets. *Journal of Composites for Construction, 16*(2), 207–216. https://doi.org/10.1061/(ASCE)CC.1943-5614.0000255
Yang, I. H., Joh, C., & Kim, B. S. (2010). Structural behavior of ultra high performance concrete beams subjected to bending. *Engineering Structures, 32*(11), 3478–3487. https://doi.org/10.1016/j.engstruct.2010.07.017
Yang, J. Q., Feng, P., Liu, B., Wang, H., Zhao, W., & Hu, L. (2022). Strengthening RC beams with mid-span supporting pre-stressed CFRP plates: An experimental investigation. *Engineering Structures, 272*, 115022. https://doi.org/10.1016/j.engstruct.2022.115022
Yang, J. Q., Smith, S. T., Wang, Z., & Lim, Y. Y. (2018). Numerical simulation of FRP-strengthened RC slabs anchored with FRP anchors. *Construction and Building Materials, 172*, 735–750. https://doi.org/10.1016/j.conbuildmat.2018.03.133
Yoo, D. Y., Kim, S. W., & Park, J. J. (2017). Comparative flexural behavior of ultra-high-performance concrete reinforced with hybrid straight steel fibers. *Construction and Building Materials, 132*, 219–229. https://doi.org/10.1016/j.conbuildmat.2016.11.104
Yoo, D. Y., & Moon, D. Y. (2018). Effect of steel fibers on the flexural behavior of RC beams with very low reinforcement ratios. *Construction and Building Materials, 188*, 237–254. https://doi.org/10.1016/j.conbuildmat.2018.08.099
Zhang, S. S., Teng, J. G., & Yu, T. (2013). Bond–slip model for CFRP strips near-surface mounted to concrete. *Engineering Structures, 56*, 945–953. https://doi.org/10.1016/j.engstruct.2013.05.032

Roba Osman is a MSc student in Menoufia University Faculty of Engineering, Egypt.

Ahmed Elkhouly is a Lecturer in Menoufia University Faculty of Engineering, Egypt.

Boshra Eltaly is a Professor in Menoufia University Faculty of Engineering, Egypt.

Mohamed H. Zakaria is a Lecturer in Kafrelsheikh University Faculty of Engineering, Egypt.